AD-A035 486 OHIO STATE UNIV RESEARCH FOUNDATION COLUMBUS F/G 21/2
IGNITION, COMBUSTION, DETONATION, AND QUENCHING OF REACTIVE MIX--ETC(U)
SEP 76 R EDSE, O DHIMAN, E MARASCO AF-AFOSR-2511-73
UNCLASSIFIED AFOSR-TR-77-0059 NL

1 OF 2
AD A035486

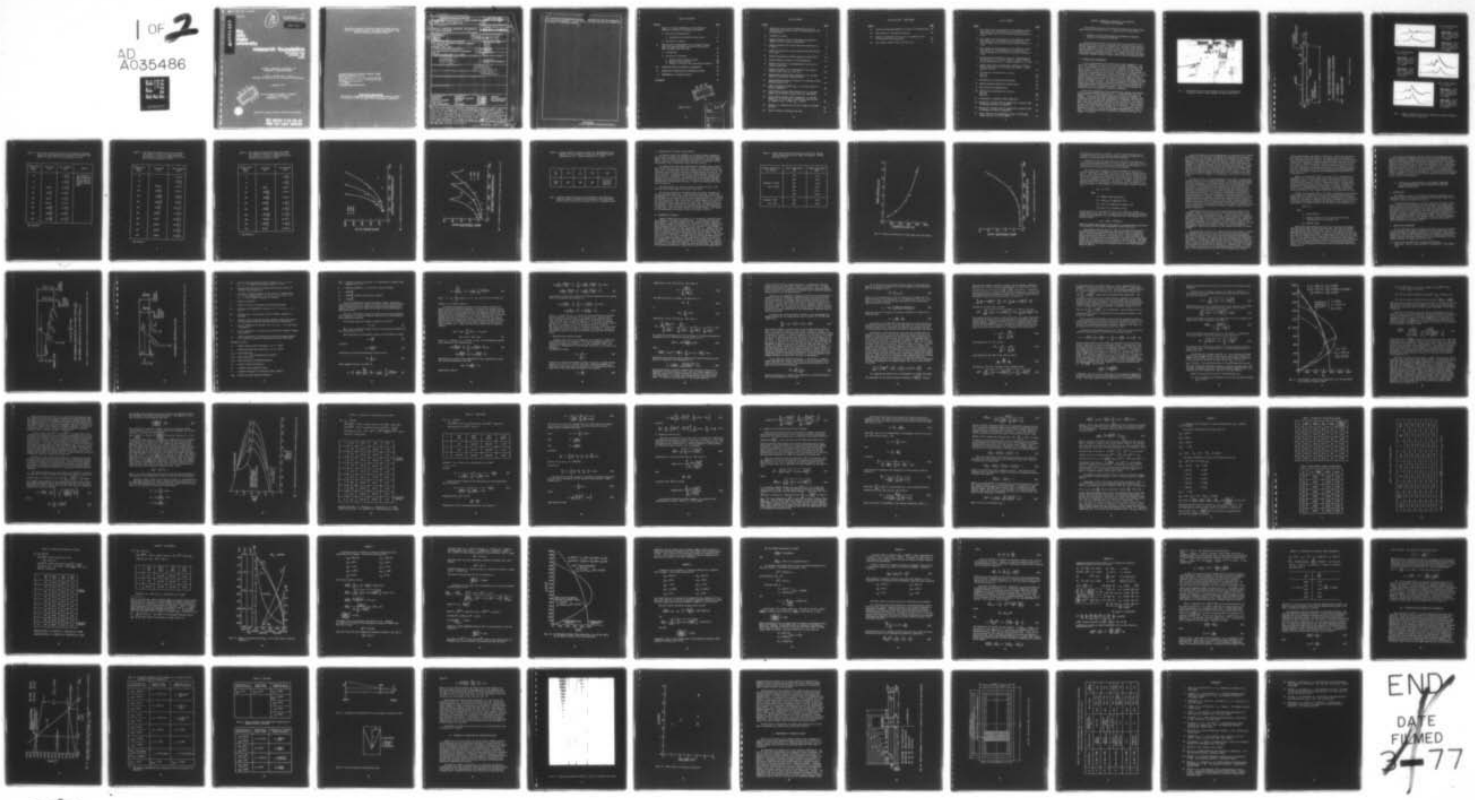

END
DATE FILMED
2-77

END
DATE FILMED
2-77

CONT

AFOSR-TR

12

RF Project 3641
Interim Technical Report

AFOSR 73-2511

the ohio state university
research foundation
1314 kinnear road
columbus, ohio
43212

IGNITION, COMBUSTION, DETONATION, AND QUENCHING OF REACTIVE MIXTURES

R. Edse, O. Dhiman, and E. Marasco
Department of Aeronautical and Astronautical Engineering

September 1976

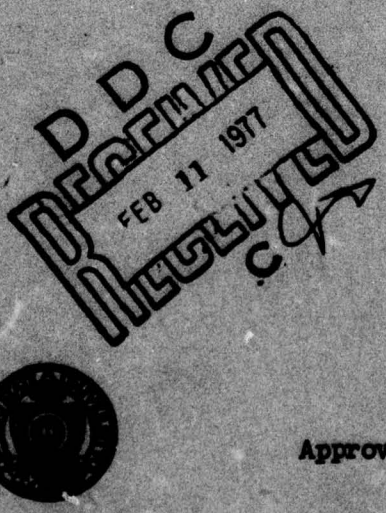

AIR FORCE OFFICE OF SCIENTIFIC RESEARCH
Bolling Air Force Base
Washington, D. C. 20332

Approved for public release; distribution unlimited.

Qualified requestors may obtain additional copies from the Defense Documentation Center, all others should apply to the National Technical Information Service.

AIR FORCE OFFICE OF SCIENTIFIC RESEARCH (AFSC)
NOTICE OF TRANSMITTAL TO DDC
This technical report has been reviewed and is approved for public release IAW AFR 190-12 (7b).
Distribution is unlimited.
A. D. BLOSE
Technical Information Officer

UNCLASSIFIED

SECURITY CLASSIFICATION OF THIS PAGE (When Data Entered)

REPORT DOCUMENTATION PAGE	READ INSTRUCTIONS BEFORE COMPLETING FORM
1. REPORT NUMBER: AFOSR-TR-77-0059	2. GOVT ACCESSION NO. / 3. RECIPIENT'S CATALOG NUMBER
4. TITLE (and Subtitle): IGNITION, COMBUSTION, DETONATION, AND QUENCHING OF REACTIVE MIXTURES	5. TYPE OF REPORT & PERIOD COVERED: INTERIM technical rept. 1 Apr 1975 — 31 Mar 1976
	6. PERFORMING ORG. REPORT NUMBER
7. AUTHOR(s): RUDOLPH EDSE, O. DHIMAN, E. MARASCO	8. CONTRACT OR GRANT NUMBER(s): AF-AFOSR-2511-73
9. PERFORMING ORGANIZATION NAME AND ADDRESS: THE OHIO STATE UNIVERSITY RESEARCH FOUNDATION, 1314 KINNEAR ROAD, COLUMBUS, OHIO 43212	10. PROGRAM ELEMENT, PROJECT, TASK AREA & WORK UNIT NUMBERS: 681308, 9711-02, 61120F
11. CONTROLLING OFFICE NAME AND ADDRESS: AIR FORCE OFFICE OF SCIENTIFIC RESEARCH/NA, BLDG 410, BOLLING AIR FORCE BASE, D C 20332	12. REPORT DATE: Sep 76
	13. NUMBER OF PAGES: 78
14. MONITORING AGENCY NAME & ADDRESS (if different from Controlling Office): 84p.	15. SECURITY CLASS. (of this report): UNCLASSIFIED
	15a. DECLASSIFICATION/DOWNGRADING SCHEDULE

16. DISTRIBUTION STATEMENT (of this Report): 9711

Approved for public release; distribution unlimited. 02

17. DISTRIBUTION STATEMENT (of the abstract entered in Block 20, if different from Report)

18. SUPPLEMENTARY NOTES

19. KEY WORDS (Continue on reverse side if necessary and identify by block number)

DEFLAGRATION	TRANSITION	COMBUSTION	SCRAMJET
DETONATION	UNCONFINED EXPLOSIVE	EQUILIBRIUM	FUEL CONSUMPTION
INDUCTION DISTANCE	HYDROGEN	SHOCK TUBE	INJECTION ANGLE
FLAME SPEED	AIR	SHOCK DECAY	
FLAME ACCELERATION	JET MIXING	QUENCHING	

20. ABSTRACT (Continue on reverse side if necessary and identify by block number)

The detonation induction distances in hydrogen-air mixtures are greatly shortened when the initial temperature of the explosive gas mixture is reduced. A new technique has been developed to calculate the effect of mixing of different gas jets on the final properties of the gas mixture. Flame speed measurements in large, nearly unconfined hydrogen-air mixtures revealed that the flame accelerates and that the speed increases with increasing volume of the explosive mixture. A shock tube has been set up to study the effect of a flame arrestor on the strength of a normal shock wave. A rectangular combustion chamber with windows is used

LB

DD FORM 1 JAN 73 1473 EDITION OF 1 NOV 65 IS OBSOLETE

UNCLASSIFIED

SECURITY CLASSIFICATION OF THIS PAGE (When Data Entered)

267360

to investigate the mechanism of deflagra[illegible] quenching with various sponge and grid type flame arrestors. Further calcula[illegible]ons have been made to determine the performance of supersonic ramjets.

TABLE OF CONTENTS

AFOSR 73-2511

LIST OF FIGURES

LIST OF FIGURES - (CONTINUED)

LIST OF TABLES

IGNITION, COMBUSTION, DETONATION, AND QUENCHING OF REACTIVE GAS MIXTURES

(Five Different Topics of this Research Program Have Been Investigated During this Report Period -- 1 April 1975 to 31 March 1976)

I. EFFECT OF INITIAL TEMPERATURE ON THE DETONATION INDUCTION DISTANCES OF HYDROGEN-AIR MIXTURES

Although many papers have been published on the structure of one-dimensional detonation waves propagating into combustible gas mixtures at room temperature, hardly any studies have been made on the effect of initial temperature on the initiation process. Several years ago Edse and Lawrence Jr.[1] measured the detonation induction distances in low-temperature hydrogen-oxygen mixtures. The present study was undertaken to determine whether fuel-air mixtures behave like fuel-oxygen mixtures.

A. APPARATUS AND MEASUREMENTS

A 6.4 m long stainless steel tube with an inner diameter of 5 cm and a wall thickness of 0.635 cm was used for these experiments. Figure 1 is a photograph of the tube, and the locations of the probes are given in Fig. 2. The detonation tube was encased in a 0.635 cm steel jacket which was welded to the tube and insulated to the surroundings by two layers of Armstrong-Armaflex rubber, each having a thickness of 1.9 cm. A Minnesota Valley Engineering (MVE) Model VGL-160L liquid nitrogen container was used to pass liquid nitrogen through the jacket at a speed which established the desired low temperature of the combustible gas mixture in the detonation tube. This mixture contained 30% hydrogen and 70% dry air by volume. Complete mixing was established in a specially designed mixing chamber from which the mixture was transferred directly as a continuous flow to the detonation tube. Prior to this transfer the detonation tube was evacuated to remove all moisture.

The initial temperature of the combustibe gas mixture was measured by two copper-constantan thermocouples. A 0.13 mm pyrofuse wire, exploded by a 40 V ac power supply, was used to ignite the hydrogen-air mixture. Two Kistler pressure transducers were employed, together with a Tektronix Type 555 dual beam oscilloscope, to determine the detonation wave speed and to measure the pressure at two locations in each experiment. The transducers were placed at various distances from the ignitor. At least three measurements were made for each location. Three typical oscilloscope traces are shown in Figs. 3a-c. All experimental data are tabulated in Tables I, II, and III and depicted graphically in Figs. 4 and 5. The detonation induction distances as obtained from Fig. 5 are compiled in Table IV.

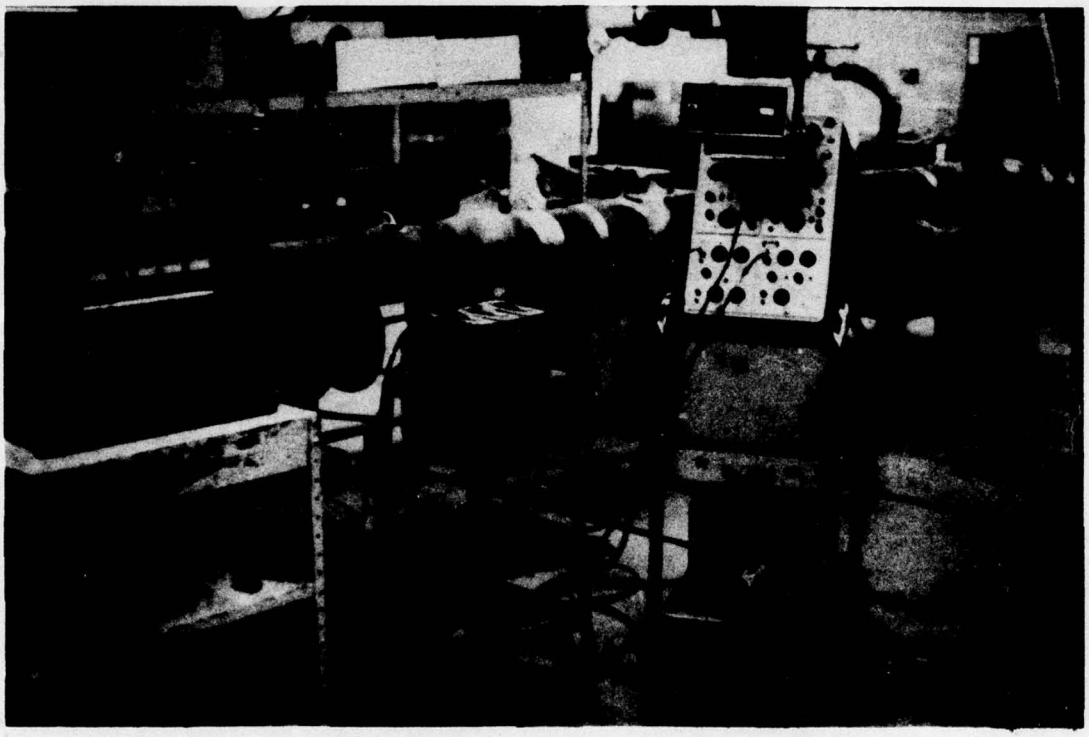

Fig. 1 - Detonation tube and other equipment used for low-temperature detonation studies of 30% hydrogen and 70% air gas mixture

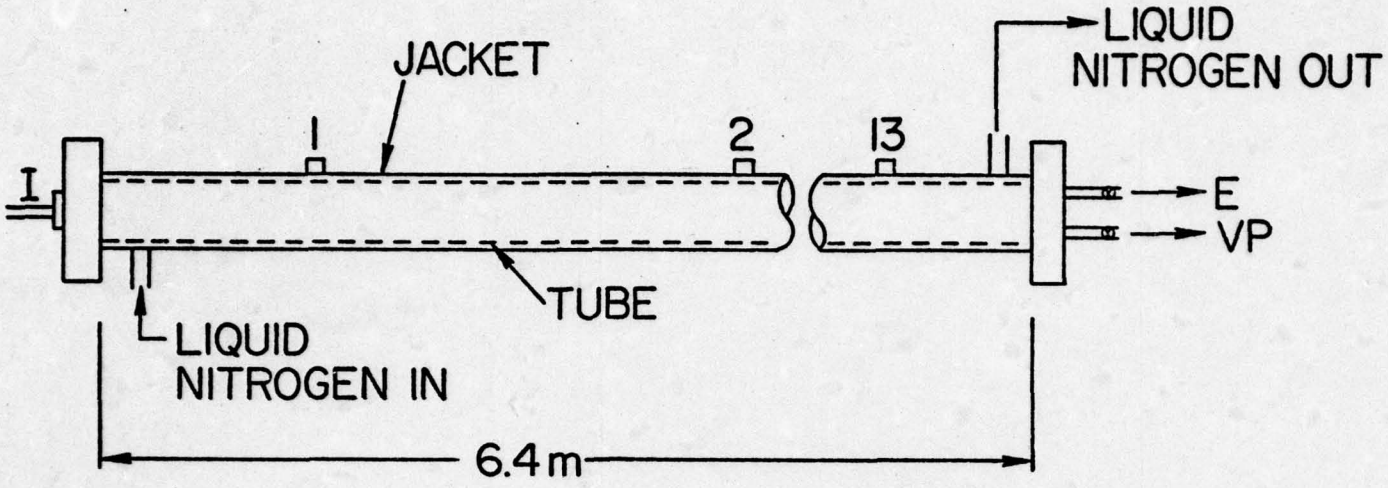

I- INLET AND IGNITER ASSEMBLY

1-13 DETECTION PROBE LOCATIONS

E- EXHAUST

VP- VACUUM PUMP

Fig. 2 - Locations of probes

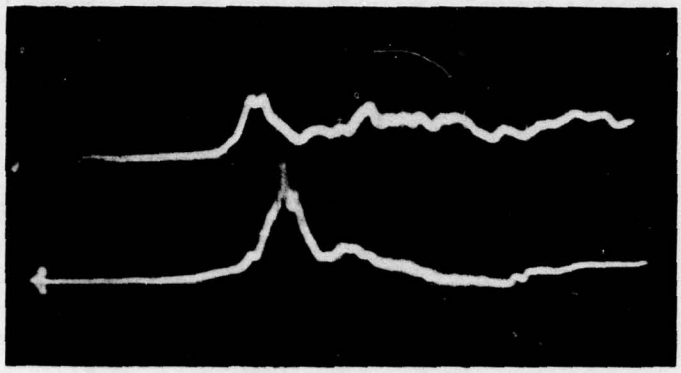

3(a) Initial Temperature = 123 K

Upper Trace: 15 cm from ignitor sweep rate = 5 ms/div vertical sensitivity = 4.4 atm/div

Lower Trace: 45 cm from ignitor sweep rate = 5 ms/div vertical sensitivity = 4.2 atm/div

3(b) Initial Temperature = 173 K

Upper Trace: 15 cm from ignitor sweep rate = 5 ms/div vertical sensitivity = 4.6 atm/div

Lower Trace: 45 cm from ignitor sweep rate = 5 ms/div vertical sensitivity = 6.3 atm/div

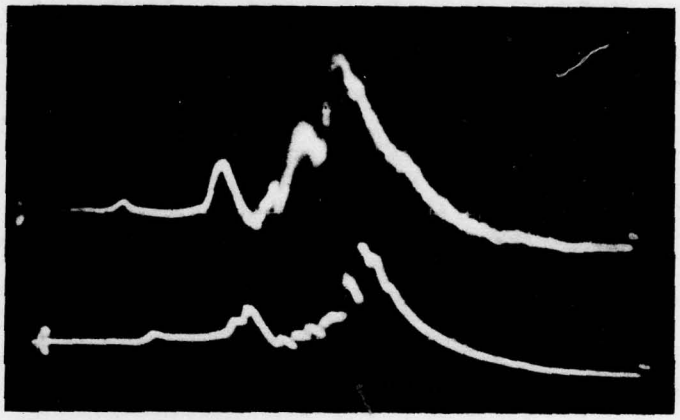

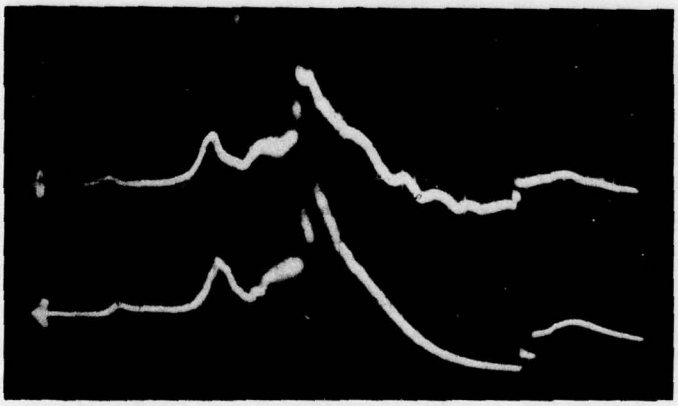

3(c) Initial Temperature = 223 K

Upper Trace: 15 cm from ignitor sweep rate = 5 ms/div vertical sensitivity = 4.6 atm/div

Lower Trace: 45 cm from ignitor sweep rate = 5 ms/div vertical sensitivity = 5.0 atm/div

Fig. 3 - Typical pressure traces in the detonation induction region at various initial temperatures

Table 1. Wave speeds and wave pressures in the detonation induction region for a 30% hydrogen in air mixture at an initial temperature of 123 K and an initial pressure of 1 atm

Distance from Ignitor (cm)	Wave Speed (m/s)	Wave Pressure (atm)	Remark
15	–	$7.3^{+2.3}_{-2.7}$	The detonation wave observed at 242 cm from the ignitor decayed further down the tube
45	–	$8.0^{+0.8}_{-0.9}$	
90	272±16	$10.3^{+0.9}_{-0.8}$	
149	500^{+75}_{-47}	$12.4^{+2.2}_{-1.1}$	
180	668±37	$25.9^{+1.7}_{-1.2}$	
242	1922±15	18.2±0.5	
302	563^{+437}_{-221}	$13.7^{+3.3}_{-4.2}$	
332	918^{+282}_{-168}	$13.0^{+2.7}_{-2.5}$	
394	717^{+222}_{-178}	$12.2^{+1.8}_{-1.4}$	

– Not measured.

Table 2. Wave speeds and wave pressures in the detonation induction region for a 30% hydrogen in air mixture at an initial temperature of 173 K and an initial pressure of 1 atm

Distance from Ignitor (cm)	Wave Speed (m/s)	Wave Pressure (atm)
15	-	4.6 ± 0.2
45	-	$6.2^{+0.3}_{-0.5}$
90	200 ± 22	6.5 ± 0.4
149	564^{+73}_{-72}	8.0 ± 0.2
180	310^{+235}_{-139}	$8.8^{+0.7}_{-0.8}$
242	933^{+100}_{-158}	$8.5^{+1.1}_{-1.3}$
302	877^{+83}_{-50}	$22.9^{+1.6}_{-1.7}$
332	1992^{+8}_{-17}	$17.4^{+0.3}_{-0.4}$
394	2000 ± 0	$18.0^{+0.4}_{-0.3}$
454	1983 ± 0	$18.0^{+0.4}_{-0.3}$
577	1972 ± 0	$18.0^{+0.4}_{-0.3}$
630	1981 ± 0	$18.0^{+0.4}_{-0.3}$

- Not measured.

Table 3. Wave speeds and wave pressures in the detonation induction region for a 30% hydrogen in air mixture at an initial temperature of 223 K and an initial pressure of 1 atm

Distance from Ignitor (cm)	Wave Speed (m/s)	Wave Pressure (atm)
15	-	$4.2^{+0.4}_{-0.2}$
45	-	$4.1^{+0.2}_{-0.0}$
90	254±4	3.6±0.0
149	387^{+203}_{-202}	3.7±0.0
180	350^{+400}_{-264}	9.9±0.6
242	1064^{+63}_{-31}	$9.8^{+0.6}_{-1.3}$
302	269^{+64}_{-45}	$14.3^{+2.0}_{-2.3}$
332	980^{+353}_{-230}	$15.1^{+2.6}_{-0.5}$
394	469±200	22.2±0.7
454	1987^{+13}_{-12}	$17.6^{+0.5}_{-0.6}$
630	2012±0	17.8±0.0

- Not measured.

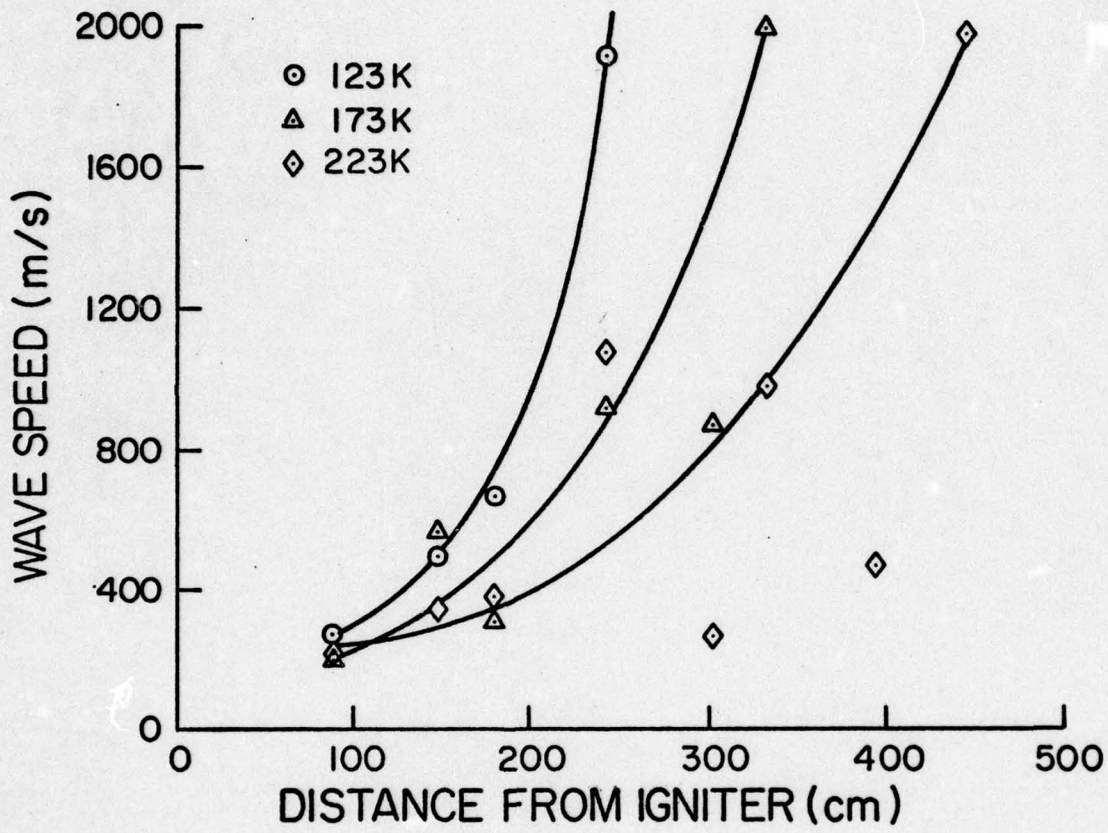

Fig. 4 - Graphic presentation of wave speed data from Tables 1, 2, and 3

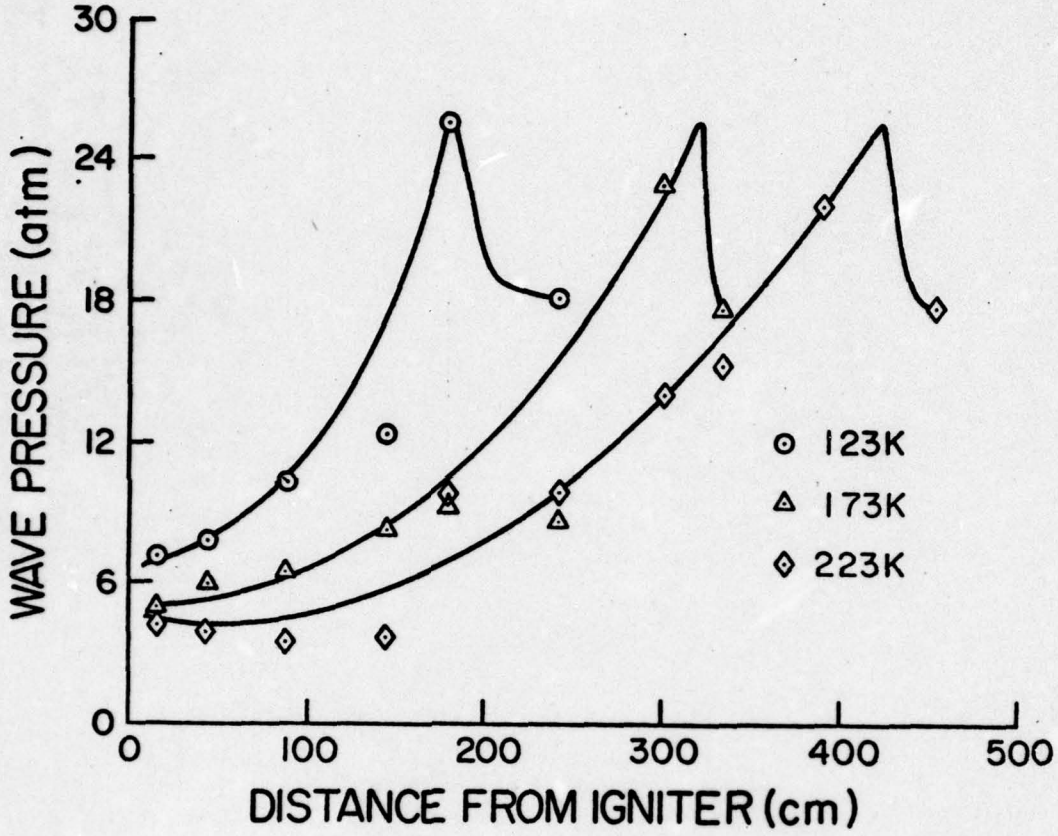

Fig. 5 - Graphic presentation of wave pressure data from Tables 1, 2, and 3

Table 4. Average induction distances (d_{ind}) in a 30% hydrogen in air mixture in a 6.4 m long, 5 cm I.D. tube at various initial temperatures (T_i): Initial Pressure, P_i = 1 atm

T_i (K)	123	173	223	295
d_{ind} (cm)	230	332	450	No Detonation was observed

Note: Induction distance (d_{ind}) has been defined as the distance between the source of ignition and that point in the tube where the wave first travels at the speed of the C.J. detonation wave.

1. Determination of Normal Burning Speeds

In order to assess the influence of the normal flame propagation rate on the transition from deflagration to detonation the flame propagation rates of hydrogen-air mixtures were measured at various temperatures. By cooling and heating the gas mixture it was possible to make measurements over a temperature range from 123 to 784 K.

At temperatures above room temperature the straight burner tube as well as the individual gas flows were heated. The hot gases were introduced into a mixing chamber which was connected to the heated 70 cm long stainless steel burner tube having an internal diameter of 0.458 cm. To avoid flash-back a hydrogen-rich mixture (53.6% hydrogen and 46.4% air) had to be used. Photographs of the flames were taken at original size on Kodak Plus-X 35 mm film. The temperature of the unburned (heated) hydrogen-air mixture was measured at the exit of the burner tube with a chromel-alumel thermocouple just prior to ignition and subsequent exposure of the film.

The flame speeds, u_f, given in Table V and shown in Fig. 6, are based on the average angle of the inner flame cone.

For the measurements at low temperatures the burner consisted of a 70 cm long copper tube with a 0.635 cm internal diameter. Mixing was accomplished in a coiled copper tube with an outside diameter of 0.635 cm. The diameter of the coils was 10 cm and the spacing was 1.3 cm. In order to avoid flash-back a small nozzle with an inside diameter of 0.3175 cm was silver-soldered to the tip of the burner tube. With this nozzle it was possible to make flame speed measurements with 30% hydrogen and 70% air mixtures. Both the burner tube and the mixing coil were immersed in a large Dewar vessel partially filled with liquid nitrogen. The results of the measurements are given in Table V and shown in Fig. 6.

B. DISCUSSION OF RESULTS

Figure 5 shows the wave pressure in the detonation induction region as a function of distance from the ignitor. On the basis of previous measurements[1] it has been assumed that the maximum pressure attained in the induction region is practically the same for all initial temperatures. These pressures were also observed in a 42 m long and 7.5 cm internal diameter detonation tube at room temperature (Fig. 7). However, the tube used for the measurements at low temperatures was not long enough to permit the formation of a stable detonation wave when the mixture was initially at room temperature. By comparing the results of Fig. 7 with those shown in Fig. 5, it can be concluded that the pressure-distance profile within the induction region at room temperature is similar to those at low temperatures. The pressure overshoot as indicated in Ref. 1, which is attributed to either shock merging[2] or to the boundary layer type initiation,[3] is also observed, before the onset of detonation. The detonation induction distances are significantly reduced as the temperature of

Table 5. Normal flame speed of hydrogen-air mixtures at various initial temperatures by the flame cone method: Initial Pressure = 1 atm

Mixture Composition (by volume)	Initial Temperature (K)	Normal Flame Speed (m/s)
Hydrogen = 53.6% Air = 46.4%	123	1.40
	290	2.64
	523	5.09
	620	6.24
	755	11.71
	784	12.18
Hydrogen = 30% Air = 70%	123	1.27
	290	2.40

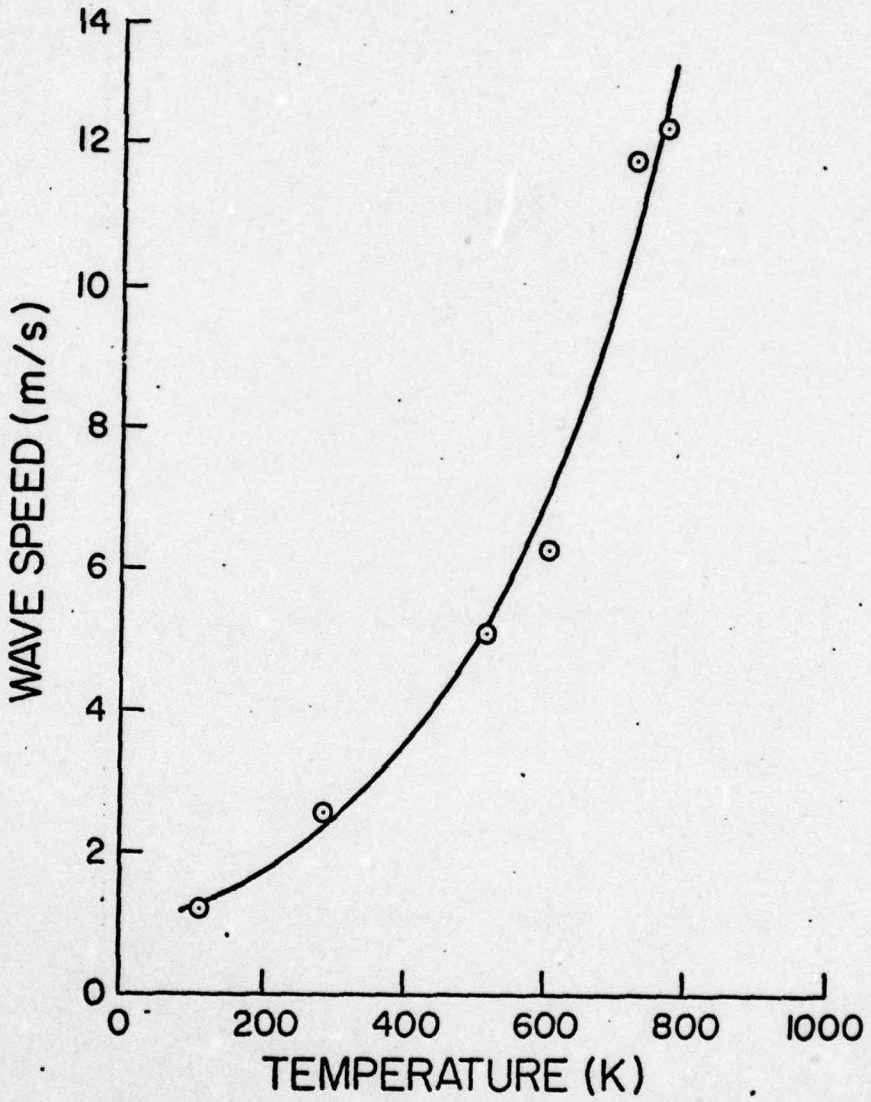

Fig. 6 - Graphic presentation of flame speed data from Table 5

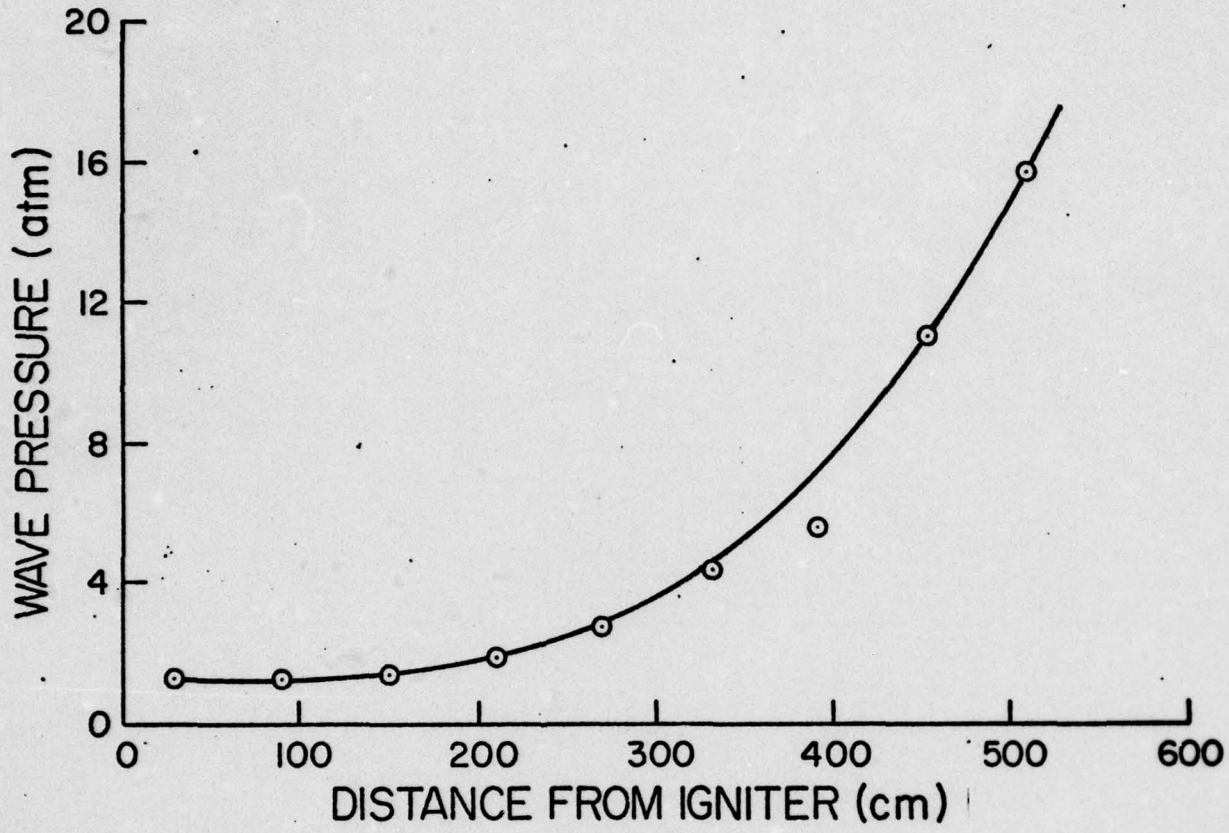

Fig. 7 - Pressure-distance profile at room temperature

the initial gas mixture is reduced. At 123 K the detonation wave is already formed 230 cm away from the ignitor whereas no detonation was observed at room temperature in this tube (Table IV).

Although at 123 K the detonation wave was formed after 230 cm of travel of the deflagration wave, it was not stable. Apparently heat losses to the cold walls of the tube are responsible for this decay. At 173 and 223 K this decay of the wave was not observed.

The normal flame propagation rates of hydrogen-air mixtures at various temperatures are compiled in Table V and depicted graphically in Fig. 6. These data reveal very clearly that the initial temperature of the gas has a substantial influence on the burning speed of this gas mixture. This observation has also been reported by Duggar and Heimel[4] for various hydrocarbon-air mixtures. The results, as shown in Fig. 6 and given in Table V for hydrogen and air mixtures, follow an empirical relationship which is quite similar to that developed by Heimel and Weast[4]; i.e.,

$$u_f = B + C \cdot T_i^{\,n} \ ,$$

where

u_f = laminar flame speed (m/s) ,

T_i = initial gas temperature (K) ,

B, C, and n are empirical constants, and

the value of n is between 2 and 3.

In the present case the values of B and C are 1.128 and 0.000018, respectively, and the value of n is taken to be 2, so that the relationship between flame propagation rate and temperature for a 30% hydrogen in air mixture becomes

$$u_f = 1.128 + 0.000018 \cdot T_i^2 \ .$$

Thus the laminar flame speed of this mixture is approximately proportional to the square of the absolute temperature of the initial gas.

The question that now arises is "How can the detonation induction distances decrease significantly when the flame speeds are reduced so much?" Edse and Lawrence Jr.[1] pointed out that: after a combustible gas mixture has been ignited in the confines of a detonation tube, the greater the resistance of the unburned gas to the motion of the expanding burned gas, the higher will be the pressure of the burned gas. Thus moderately strong compression waves are generated in the unburned gas which merge rapidly and thus form a detonation wave at a very short distance from the ignitor.

Since the resistance of the unburned gas is a function of its density and friction at the tube wall, the greater the density of the unburned gas the more it will keep the burning gas from expanding so that pressure waves are formed more readily and thus lead to a rapid transition from deflagration to detonation. Since the lowering of the initial gas temperature at a constant pressure (1 atm) increases the density of the gas and hence the resistance to the flow of the expanding burned gas, rather strong compression waves are generated right at the onset of ignition. This fact is evidenced by the pressure traces shown in Fig. 5. At 123 K and at 15 cm from the ignitor the pressure rise is already of the order of 8 atm, at 173 K it amounts to 5 atmospheres, and at 223 K it is only 4 atm.

As shown in Fig. 7, at room temperature the pressure is essentially constant even up to 150 cm from the ignitor. Thus, these strong compression waves generated at low temperature increase the pressure and temperature of the unburned gas much more rapidly than at room temperature. In addition, the reflection of the precompression shock from the tube walls and the downstream end of the tube increase the temperature and pressure of the unburned gas even further by increasing the strength of the precompression shock. An increase in temperature and pressure of the compressed but unburned gas increases the burning velocity of the combustion wave very rapidly. Furthermore, when the reflection of rather strong compression waves passes through the combustion wave a large increase of the flame surface occurs,[5] so that rather turbulent flames are produced which also lead to a significant increase of the burning rate.[6] Also, as pointed out by Brinkley and Lewis,[7] the effect of reflected waves on the acceleration of the flame is much more effective than the incremental acceleration.

According to Karlovitz,[8] a very strong turbulent wrinkling of the combustion surface can be produced by a very strong shock wave so that a detonation wave is formed more quickly. Thus as long as the burning speed of the initial gas mixture is large enough to maintain a combustion wave, the much higher rise in pressure and temperature of the compressed but unburned gas due to the lowering of its temperature along with the generation of turbulence (as explained above), is always going to increase the burning rates to a much greater extent than at room temperature. Consequently a significant reduction of the induction distance is accomplished.

To explain why at 123 K a C.J. detonation wave once formed is unable to propagate further down the tube with a constant speed and pressure, the stability and structure of the so-called self-sustained detonation wave will be examined. Many papers have been published after Zeldovitch,[9] von Neuman,[10] and Döring[11] proposed their model regarding the stability and structure of self-sustaining detonation waves. According to the ZND model, a gaseous detonation wave consists of a shock wave which traverses the unreacted gas mixture and is followed by a reaction zone. The chemical changes are initiated in the high-temperature gas behind the shock wave. It is assumed that at the tail of the reaction zone, the gas

reaches thermodynamic and chemical equilibrium. The energy released by the combustion of the fuel supports the propagation of the shock wave. Thus, the detonation wave (that is, the combination of the shock and combustion waves) possesses a self-sustaining or stable character and propagates with a constant speed and pressure, commonly referred to as the C.J. velocity and C.J. pressure. The detonation wave speed and pressure are independent of the chemical kinetics of the combustion reaction and they are governed only by the fluid mechanical and thermodynamical laws. The ZND model is based on the one-dimensional structure of the detonation wave.

However, as observed by Fay[12] the structure of a self-sustained detonation wave is strongly influenced by the chemical kinetics of the combustion process. It is quite certain[13] that the wave front of all self-sustaining detonation waves is three-dimensional. The one-dimensional flow behind a plane detonation front is usually disturbed by the occurrence of three-dimensional oscillations in the gas. Martin and White,[14] using interferometry to investigate near limit detonations, found convolutions in the reacting gases which they attributed to spin.

Döring[11] has suggested that at the limit of detonability rarefaction waves, generated by cooling at the wall of the tube, may penetrate far enough into the reaction zone to quench the detonation wave. Sokolik[15] taking into consideration Döring's idea that a rarefaction wave is formed at the tube wall during cooling of the hot gases in the reaction zone, postulated the following criterion for the decay of the detonation wave:

$$d/2c < t_r ,$$

where

d = tube diameter,

c = speed of sound (i.e., the speed with which the rarefaction wave will travel), and

t_r = reaction time.

Zeldovitch[9] also considers the heat losses from the hot boundary layer to the cold wall of the detonation tube. This heat loss lowers the temperature in the reaction zone, which causes a decrease of the chemical reaction rates and thus may lead to an incomplete liberation of heat from the combustion process. Consequently the strength of the shock wave will be reduced, which, in turn, will reduce the reaction rate still more. As the reaction rate is decreased the thickness of the reaction zone is increased. The effect of thermal losses as explained by Döring,[11] Sokolik,[15] and Zeldovitch[9] applies only to one-dimensional detonation waves. The three-dimensional analysis of the wave includes heat losses automatically.

Then after the detonation wave has decayed to a deflagration wave, suitable conditions of temperature and pressure farther down the tube may cause the flame to accelerate again and form another shock wave which results in the formation of a second stable detonation wave. The high temperature and pressure may be caused by reflection of the initial shock wave from the closed end of the tube. This explanation is in agreement with the data given in Table I; in one experiment a C.J. detonation was observed at 577 cm from the ignitor after the decay of the first wave which was formed at 230 cm from the ignitor. It appears that this behavior of the detonation wave occurs only at 123 K because of the higher thermal losses at this low temperature.

II. CALCULATION OF THERMODYNAMIC AND GAS-DYNAMIC PROPERTIES OF A ONE-DIMENSIONAL GAS FLOW TO WHICH ONE OR MORE DIFFERENT GASES ARE ADDED

A. INTRODUCTION

The addition of gases to a primary flow through a duct may be accomplished either with an increase in duct area as shown in Fig. 8 or in a constant area duct as depicted in Fig. 9.

In the following analysis it will be assumed that the flow is adiabatic relative to the environment and that there are no viscous interactions between the flow and the walls of the duct. The calculation of the length of the channel required to produce a completely homogeneous gas mixture will not be included in this analysis because this problem involves the complex nonequilibrium and rate phenomena of diffusion, heat transfer, momentum exchange, and chemical changes. The inclusion of these relationships leads to very complex, and, in all but the simplest, highly idealized cases only to approximate, equations which cannot be solved rigorously at the present time.

B. DERIVATION OF EQUATIONS

For the derivation of the equations which must be used to calculate the thermodynamic and gasdynamic properties of the uniform final flow (subscript m when no chemical changes occur and subscript c when chemical changes have occurred and produced a mixture in chemical equilibrium) from the initial conditions (subscript i) of the unmixed gases, the following notations and definitions will be used:

A_o = area of duct through which the primary flow passes.
Subscript 0 (zero) is used to denote all properties of the primary flow

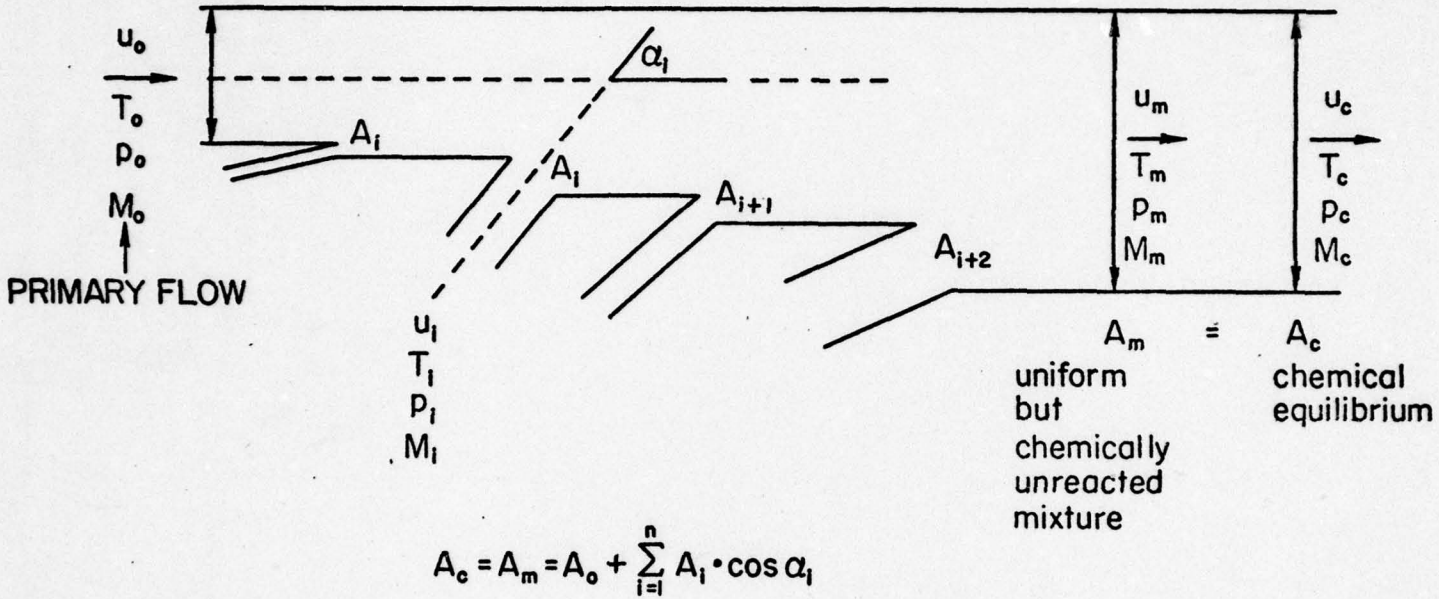

$$A_c = A_m = A_o + \sum_{i=1}^{n} A_i \cdot \cos \alpha_i$$

FOR TANGENTIAL INJECTION ALL $\alpha_i = 0$ AND THUS $A_m = \sum_{i+0}^{n} A_i$

FOR NORMAL INJECTION ALL $\alpha_i = \pi/2$ AND THUS $A_m = A_o$

Fig. 8 - Addition of gases to a one-dimensional flow with increase of duct area

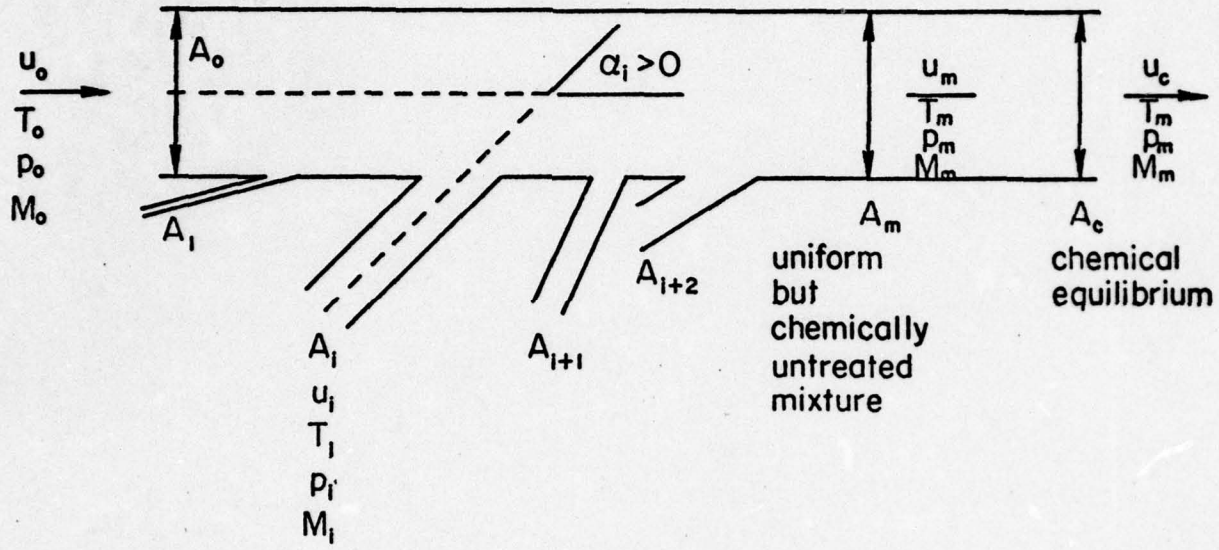

Fig. 9 - Addition of gases to a one-dimensional flow without change of duct area ($A_c = A_m = A_o$)

A_i = area of injector through which the species is (i = 1, or 2, 3, ...n) added to the primary flow (i - 0) at

α_i = angle between direction of primary flow and that of axis of injector carrying species i

i = subscript to denote chemical species of gases, primary flow (i = 0) and injected gases. i = 1, 2, 3 .....n or i = 1, 2, 3, ...z when chemical changes are involved

n = number of injectors

z = number of species in mixture in chemical equilibrium

$\mathfrak{m}_i$ = molecular mass (kg/kmol) of species i (i = 0, 1, 2, 3, ...n or z)

$\mathfrak{m}_m$ = molecular mass of gas mixture when no chemical changes are involved

$\mathfrak{m}_c$ = molecular mass of gas mixture when chemical changes have occurred and complete chemical equilibrium has been established

T_i = static temperature of species i (i = 0, 1, 2, ...n) just prior to mixing (K)

T_m = static temperature of uniform final flow when no chemical changes have occurred

T_c = static temperature of uniform final flow when chemical changes have occurred and chemical equilibrium has been established

Similarly we have:

p = static pressure with subscripts i, m, or c (N/m^2)

u = linear gas speed with subscripts i, m, or c (m/s)

$\eta_{i,m}$ = mole fractions
$x_{i,m}$ = mass fractions
} of unreacted gas mixture

$\eta_{i,c}$ = mole fractions of reacted gas mixture

ν_i = number of moles of species i

H = absolute molar enthalpy (J/mol)

h = absolute enthalpy of a unit mass [J/kg = $(m/s)^2$]

$E_{o,i}$ = molar zero point energy of species i

$\Delta H_{f,i}^{T}$ = formation enthalpy of species i at temperature T (J/kmol) from elements at T = 0 K.

$\mathcal{R}$ = 8314.33 (J/kmol·K) = universal gas constant (J/kg·K)

$R_i = (\mathcal{R}/m_i)$

$R_m = (\mathcal{R}/m_m)$ } specific gas constants (J/kg·K)

$R_c = (\mathcal{R}/m_c)$

The three fundamental, unknown properties (namely, temperature, speed, and pressure) of the flow of the mixture can be calculated from equations derived from the conservation laws of mass, momentum, and energy, and the equation of state in the forms in which they apply to this kind of flow.

The first relationship between the known initial and the unknown final conditions of a flow is obtained from the law of conservation of mass (continuity equation).

For the mass flow rate through a channel we can write

$$\dot{m} = \rho u A \tag{1}$$

When ρ and u represent average values of the density and speed over the cross-sectional area A.

Upon elimination of the density by means of the equation of state

$$\rho = \frac{p\mathcal{M}}{\mathcal{R}T} , \tag{2}$$

we obtain

$$\dot{m} = \frac{p \cdot \mathcal{M} \cdot u \cdot A}{\mathcal{R} \cdot T} \tag{3}$$

According to the law of conservation of mass we have

$$\dot{m} = \sum_{i=0}^{n} \dot{m}_i , \tag{4}$$

which together with Eq. (3) leads to

$$p_m = \frac{\dot{m}}{A_m} \cdot \frac{\mathcal{R}T_m}{\mathcal{M}_m u_m} = \frac{\sum_{i=0}^{n} m_i}{\mathcal{M}_m u_m} \cdot \frac{\mathcal{R}T_m}{A_m} = \frac{T_m}{u_m \mathcal{M}_m A_m} \cdot \sum_{i=0}^{n} \frac{p_i \mathcal{M}_i u_i A_i}{T_i} \tag{5}$$

or

$$p_c = \frac{\sum_{i=0}^{n} \dot{m}_i}{m_c u_c A_m} \cdot \mathcal{R} T_c = \frac{T_c}{u_c m_c A_m} \sum_{i=0}^{z} \frac{p_i m_i u_i A_i}{T_i} \tag{6}$$

where $A_m = A_o + \sum_{i=1}^{n} A_i \cos\alpha_i$ or $A_m = A_o$ for the case of normal injection, or as shown in Fig. 9.

The second relationship between known and unknown variables is based on the conservation of momentum. As long as all viscous interactions between the fluid and the walls of the duct and injectors through which they pass can be disregarded, the total momentum of the fluid, or more precisely its momentum flux at any cross sectional area in the duct, is made up of two contributions; i.e., (1) the momentum flux, $\dot{m}u$, resulting from the motion of the fluid as a whole, and (2) the momentum flux caused by the random motion of the individual molecules of the gas which is equal to the product of the static pressure and the channel cross-sectional area. Thus, for such flows, conservation of momentum leads to

$$\dot{m}_o u_o + A_o p_o + \sum_{i=1}^{n} \left(m_i u_{i,x} + A_{i,x} p_i \right) =$$

$$\dot{m} u_m + A_m p_m = \dot{m} u_c + A_m p_c \ . \tag{7}$$

With $A_{i,x} = A_i \cos\alpha_i$, $u_{i,x} = u_i \cos\alpha_i$ and Eq. (3) the momentum equation can be written in the following form:

$$A_o p_o \left(\frac{m_o u_o^2}{\mathcal{R} T_o} + 1 \right) + \sum_{i=1}^{n} A_m p_i \left(\frac{m_i u_i^2}{\mathcal{R} T_i} + 1 \right) \cos\alpha_i = \tag{8}$$

$$A_m p_m \left(\frac{m_m u_m^2}{\mathcal{R} T_m} + 1 \right) = A_m p_c \left(\frac{m_c u_c^2}{\mathcal{R} T_c} + 1 \right) \ .$$

The areas A_o, A_i, and A_m can be removed from this expression by using the continuity equation in the form

$$A_o p_o = \dot{m}_o \frac{\mathcal{R} T_o}{m_o u_o} \ , \text{ etc.}$$

Substitution leads to

$$\dot{m}_o \frac{\mathcal{R}T_o}{\mathcal{M}_o u_o}\left(\frac{\mathcal{M}_o u_o^2}{\mathcal{R}T_o}+1\right)+\sum_{i=1}^{n} m_i \frac{\mathcal{R}T_i}{\mathcal{M}_i u_i}\left(\frac{\mathcal{M}_i u_i^2}{\mathcal{R}T_i}+1\right)\cos\alpha_i =$$

$$\dot{m}\frac{\mathcal{R}T_m}{\mathcal{M}_m u_m}\left(\frac{\mathcal{M}_m u_m^2}{\mathcal{R}T_m}+1\right)=\dot{m}\frac{\mathcal{R}T_c}{\mathcal{M}_c u_c}\left(\frac{\mathcal{M}_c u_c^2}{\mathcal{R}T_c}+1\right). \qquad (9)$$

Upon division of the whole equation by $\dot{m}$ and by factoring out the second term in each parenthesis we arrive at

$$x_o u_o\left[\frac{\mathcal{R}T_o}{\mathcal{M}_o u_o^2}+1\right]+\sum_{i=1}^{n} x_i u_i\left[\frac{\mathcal{R}T_i}{\mathcal{M}_i u_i^2}+1\right]\cos\alpha_i =$$

$$u_m\left[\frac{\mathcal{R}T_m}{\mathcal{M}_m u_m^2}+1\right]=u_c\left[\frac{\mathcal{R}T_c}{\mathcal{M}_c u_c^2}+1\right], \qquad (10)$$

where $x_o = (m_o/m)$ and the $x_i = (m_i/m)$ are the so-called mass fractions of the individual constituents of the initial flow. Equation (10), which satisfies both the law of conservation of momentum and that of mass, contains only two unknowns (namely, T_m and u_m) when no chemical changes occur, since in this case $\mathcal{M}_m$ can be calculated readily; whereas the final gas composition must be determined first to calculate $\mathcal{M}_c = \sum \eta_{i,c}\,\mathcal{M}_i$, where the $\eta_{i,c}$ are the mole fractions of the individual constituents of the final mixture in chemical equilibrium. Because of the greater complexity of these calculations this case will be treated later.

1. Mixing Without Chemical Changes

Turning now to the case of chemically inert mixtures, we find that the molecular mass of the mixture, $\mathcal{M}_m$, can be calculated readily by means of the known mass fraction, x_i, of the individual flows. Frequently it is advantageous to use the mole fractions, η_i, for these calculations.
By definition we have

$$\eta_i = \frac{\dot{\nu}_i}{\sum_{i-0}^{n} \dot{\nu}_i}, \qquad (11)$$

where the $\dot{\nu}_i$ represent the number of moles of species i passing through channel A_i (i = 0, 1, 2...n) per unit time. These mole numbers are equal to the mass flow rate, $\dot{m}_i$, divided by the corresponding molecular mass, $\mathcal{M}_i$, of the constituent according to the equation

$$\dot{\nu}_i = \frac{\dot{m}_i}{\mathcal{M}_i}. \qquad (12)$$

Substitution of Eq. (12) into Eq. (11) leads to

$$\eta_i = \frac{\left(\frac{m_i}{\mathcal{M}_i}\right)}{\sum_{i=0}^{n} \left(\frac{m_i}{\mathcal{M}_i}\right)_i} \quad . \tag{13}$$

The molecular mass of a mixture, by definition, is

$$\mathcal{M}_m = \frac{\dot{m}}{\dot{\nu}} \tag{14}$$

or

$$\mathcal{M}_m = \sum_{i=0}^{n} \eta_i \mathcal{M}_i \quad . \tag{15}$$

Substitution of Eq. (13) into Eq. (15) leads to

$$\mathcal{M}_m = \frac{\sum_{i=0}^{n} \left(\frac{\dot{m}_i}{\mathcal{M}_i}\right) \mathcal{M}_i}{\sum_{i=0}^{n} \left(\frac{\dot{m}_i}{\mathcal{M}_i}\right)} = \frac{\sum_{i=0}^{n} m_i}{\sum_{i=0}^{n} \left(\frac{\dot{m}_i}{\mathcal{M}_i}\right)} = \frac{\dot{m}}{\sum_{i=0}^{n} \left(\frac{m_i}{\mathcal{M}_i}\right)} = \frac{1}{\sum_{i=0}^{n} \left(\frac{x_i}{\mathcal{M}_i}\right)} \quad . \tag{16}$$

For numerical calculations Eq. (10) is written as an equation giving the temperature T_m as a function of the gas speed u_m; i.e.,

$$T_m^{(M-C)} = \frac{u_m \left(u_{m,max}^{(M-C)} - u_m \right)}{R_m} \quad , \tag{17}$$

where

$$u_{m,max}^{(M-C)} = x_o u_o \left(1 + \frac{R_o T_o}{u_o^2}\right) + \sum_{i=1}^{n} x_i u_i \left(1 + \frac{R_i T_i}{u_i^2}\right) \cos\alpha_i \quad .$$

Alternately, Eq. (10) can also be written as an equation giving the gas speed as a function of the temperature; i.e.,

$$u_m = \frac{1}{2} u_{m,max}^{(M-C)} \pm \sqrt{\left[\frac{1}{2} u_{m,max}^{(M-C)}\right]^2 - R_m T_m} \quad . \tag{18}$$

The superscript M-C is used to indicate that numerical values of the temperature calculated by means of Eq. (17) for certain speeds, u_m, or numerical values of the speed calculated by means of Eq. (18) for certain temperatures, T_m, satisfy only the momentum and continuity equations. To calculate the temperature T_m (or the gas speed u_m)

which satisfies also the energy equation it is necessary to use the energy equation to remove the gas speed, u_m, from Eq. (17). In other words we must obtain an equation which contains T_m as the only unknown or we must remove the temperature T_m from Eq. (18) to obtain an equation which contains u_m as the only variable.

Because of the complicated relationship between the thermodynamic functions (such as enthalpies, internal energies, and specific heats) and the temperature, a rigorous solution can be established only for calorically perfect gases [temperature-independent specific heats, see Eq. (37)]. For all other gases, even when no chemical changes occur, the final conditions (u_m, T_m, and p_m) can be calculated only by an iteration procedure. The accuracy of the results can be as good as desired. Of course, it cannot exceed that of the thermodynamic functions used in these calculations.

As long as the flow is adiabatic relative to its environment the energy equation for the mixing process can be written in the following simple form:

$$\sum_{i=0}^{n} \dot{m}_i \left(h_i + \frac{u_i^2}{2} \right) = \dot{m} \left(h_m + \frac{u_m^2}{2} \right) . \tag{19}$$

The injection angles α_i do not appear in the energy equation because they do not have any influence on the scalar property of energy. The terms representing the heat transfer between the various gas flows, which is necessary to achieve a uniform temperature, do not have to be included in the energy equation because only the final state of the gas is to be calculated. This internal transfer of energy is included implicitly in Eq. (19). It affects only the magnitudes of the two terms representing the energy of the flow; i.d., h, the enthalpy which consists of the random motion energies of the molecules plus the flow work term pv, and $(u^2/2)$, the kinetic energy due to the motion of the gas as a whole. In the same manner the viscous interactions between the various flows are taken into consideration in the momentum equation in which viscous interactions determine the relative magnitudes of the momenta due to the random motion (p) and ordered motion (ρu^2) to the total momentum which remains constant as long as wall friction is disregarded.

In Eq. (19) the absolute enthalpies, h_i, of species i (usually a single component gas; if not, such as air, it may be treated as if it were a pure gas) are related to the absolute molar enthalpies of the species by the following expression:

$$h_i^{T_i} = \frac{H_i^{T_i}}{m_i} \left[\frac{J}{kg} \right] , \tag{20}$$

where the superscript T_i denotes the temperature at which the value of the absolute enthalpy is to be taken.

On the other hand the absolute enthalpy, $h_m^{T_m}$, of a unit mass of a mixture is obtained by summing the properly weighted molar enthalpies, $H_i^{T_m}$, of the species; e.g.,

$$h_m^{T_m} = \sum_i n_{i,m} H_i^{T_m} \quad , \tag{21}$$

where T_m is the temperature of the gas mixture, which means that all constituents have this temperature. The weighting factors in Eq. (21), the $n_{i,m}$, are the so-called specific molalities of the constituents. They are defined as follows:

$$n_{i,m} = \frac{\nu_{i,m}}{m} \left[\frac{\text{moles of species i}}{\text{unit mass of mixture}} \right] , \tag{22}$$

Using Eq. (12) we can express the specific molalities in terms of the mass fractions;

$$n_{i,m} = \frac{m_i}{m \mathcal{M}_i} = \frac{x_i}{\mathcal{M}_i} \quad . \tag{23}$$

As long as only steady flows are considered it is not necessary to distinguish between mass (m_i or m) and mass flow rate ($\dot{m}_i$ or $\dot{m}$) in many of these relationships. Therefore, to simplify the notation, the dot over the properties denoting flow rates will be omitted when permissible.

Sufficiently accurate numerical values for the absolute molar enthalpies of the species, H_i^T, are not available because they can be obtained only from determinations of the molecular masses extending to at least 16 significant digits, which is many orders of magnitude beyond our present capabilities. The absolute enthalpies include the rest mass of the species, expressed in units of energy, $E_{o,i} = \mathcal{M}_{o,i} \cdot c^2$ (c = speed of light) which make the numerical values so enormously large. Since we are never interested in absolute enthalpies, because only differences appear in all equations involving enthalpy (or internal energy), the absolute values can always be replaced by properly selected relative values of enthalpy (or internal energy). When no chemical changes (which means no mass changes according to Einstein's mass-energy equivalence relationship, $\Delta e = -\Delta m \cdot c^2$) occur in the process under consideration, the absolute molar enthalpies, H_i^T, can be replaced by the sensible enthalpies, $(H-E_o)_i^T$. Thus using the relationships Eqs. (20) and (21) and introducing the sensible enthalpies, the energy equation [Eq. (19)] can be written as follows:

$$\sum_{i=0}^{n} \dot{m}_i \left[\frac{(H-E_o)_i^{T_i}}{\mathcal{M}_i} + \frac{u_i^2}{2} \right] = \dot{m} \left[\sum n_{i,m} (H-E_o)_i^{T_m} + \frac{u_m^2}{2} \right] . \tag{24}$$

For computational purposes it is advantageous to replace the sensible enthalpies by the reduced sensible enthalpies, $\left(\frac{H-E_o}{\mathcal{R}T} \right)_i^T$, because

they are more readily available in tables than the sensible enthalpies. Therefore, Eq. (24) is modified by multiplying the first term in each square bracket by the identities $\frac{\mathcal{R}T_i}{\mathcal{R}T_i}$ or $\frac{\mathcal{R}T_m}{\mathcal{R}T_m}$, respectively. Furthermore, the whole equation is divided by the mass of the mixture, m, and the specific molalities are eliminated by means of Eq. (23) to express the composition in terms of the mass fractions. We arrive at

$$\sum_{i=0}^{n} \frac{x_i}{m_i} \mathcal{R}T_i \left(\frac{H-E_o}{\mathcal{R}T}\right)_i^{T_i} + \sum_{i=0}^{n} x_i \frac{u_i^2}{2} = \sum_{i=0}^{n} \frac{x_i}{m_i} \mathcal{R}T_m \left(\frac{H-E_o}{\mathcal{R}T}\right)_i^{T_m} + \frac{u_m^2}{2} .$$

Solving for the gas speed we obtain

$$u_m^{(E)} = \sqrt{\sum_{i=0}^{n} x_i \left[u_i^2 + 2R_iT_i \left(\frac{H-E_o}{\mathcal{R}T}\right)_i^{T_i}\right] - 2R_mT_m \sum_{i=0}^{n} \frac{x_i}{m_i} \left(\frac{H-E_o}{\mathcal{R}T}\right)_i^{T_m}} \quad (25)$$

The superscript (E) is used to indicate that this gas speed, when calculated for an arbitrary value of the temperature T_m, satisfies only the energy equation. Usually its numerical value is obtained with an arbitrarily assumed temperature, T_m. The last term under the square root sign in Eq. (25) can be simplified slightly by replacing the mass fraction, x_i, by the mole fractions, η_i. According to Eq. (13) we have

$$\eta_i = \frac{\nu_i}{\sum_{i=0}^{n} \nu_i} = \frac{\frac{\dot{m}_i}{m_i}}{\sum_{i=0}^{n} \frac{\dot{m}_i}{m_i}} , \quad (26)$$

and according to Eq. (14) we have

$$m_m = \frac{\dot{m}}{\sum_{i=0}^{n} \dot{\nu}_i} = \frac{\dot{m}}{\sum_{i=0}^{n} \frac{\dot{m}_i}{m_i}} . \quad (27)$$

Upon division of Eq. (26) by Eq. (27) we obtain

$$\frac{\eta_i}{m_m} = \frac{\frac{\dot{m}_i}{m_i}}{\dot{m}} = \frac{x_i}{m_i} , \quad (28)$$

and thus Eq. (25) can be written in the following form:

$$u_m^{(E)} = \sqrt{\sum_{i=0}^{n} x_i \left[u_i^2 + 2R_iT_i \left(\frac{H-E_o}{\mathcal{R}T}\right)_i^{T_i}\right] - R_mT_m \sum_{i=0}^{n} \eta_i \left(\frac{H-E_o}{\mathcal{R}T}\right)_i^{T_m}} . \quad (29)$$

An approximate value of the gas speed, u_m, can be calculated when the expression for the temperature of the gas mixture, $T_m^{(M-C)}$, according to Eq. (17), is substituted into Eq. (29). The resulting quadratic equation in u_m may be considered to contain u_m as the only unknown because the term $\sum_{i=0}^{n} \eta_i \left(\frac{H-E_0}{\mathcal{R}T}\right)_i^{T_m}$ varies only very slightly with temperature. For calorically perfect gases the reduced sensible enthalpies are constant so that for such gases the speed of the gas mixtures can be calculated directly from the given conditions. For gases with temperature-dependent reduced sensible enthalpies the speed of the mixture can be calculated by an iteration procedure starting with a reasonable estimate of T_m so that the sum $\sum_{i=0}^{n} \eta_i \left(\frac{H-E_0}{\mathcal{R}T}\right)_i^{T_m}$ can be determined. This procedure will be developed after a general insight into the relationships between T_m and u_m has been gained.

For an efficient application of the iteration procedure and for a critical appraisal of the solution obtained by the method described above it is helpful to examine the possible range of values of T_m and u_m as given by the combined momentum and continuity equations alone [Eqs. (17) or (18)] and by the energy equation alone [Eq. (29)].

According to the momentum equation [Eq. (17)] the range of possible speeds of the gas mixture is given by the following condition:

$$0 \leq u_m \leq u_{m,max}^{(M-C)} = \left[x_0 u_0 \left(\frac{R_0 T_0}{u_0^2} + 1\right) + \sum_{i=1}^{n} x_i u_i \left(\frac{R_i T_i}{u_i^2} + 1\right) \cos\alpha_i \right] . \quad (30)$$

For gas speeds outside of this range the temperature of the gas mixture would be negative, an obviously impossible result. Therefore, the term in the square bracket of Eq. (30) represents the maximum possible speed of the gas mixture according to the momentum equation. It is obvious that $T_m^{(M-C)}$ becomes zero when $u_m = 0$ and when $u_m = u_{m,max}$. The maximum speed, $u_{m,max}^{(M-C)}$, and the specific gas constant, R_m, are constants for a given set of initial conditions (x_i, u_i, T_i, m_i, and α_i). An inspection of Eq. (17) [or (18)] reveals at once that the relationship between u_m and T_m satisfying the momentum and continuity equations simultaneously is that of a parabola and that the temperature of the gas mixture attains the largest possible value for a given set of initial conditions when $u_m = 1/2\ u_{m,max}^{(M-C)}$. Thus we have

$$T_{m,max}^{(M-C)} = \frac{\left(0.5 u_{m,max}^{(M-C)}\right)^2}{R_m} . \quad (31)$$

Furthermore, we note [see Eq. (18)] that for each possible temperature of the gas mixture there are two different speeds which the mixture may attain. This fact requires special attention; it is necessary to know

whether both solutions are physically possible and what processes they represent.

Turning now to the energy equation [Eq. (29)] we recognize at once that the range of possible speeds of the gas mixture is given by the following condition:

$$0 \leq u_m \leq \sqrt{\sum_{i=0}^{n} x_i \left[u_i^2 + 2R_i T_i \left(\frac{H-E_o}{\mathcal{R}T} \right)_i^{T_i} \right]} . \tag{32}$$

The maximum gas speed, u_m, according to the energy equation is attained when the temperature of the mixture becomes zero. Thus we write

$$\sqrt{\sum_{i=0}^{n} x_i \left[u_i^2 + 2R_i T_i \left(\frac{H-E_o}{\mathcal{R}T} \right)_i^{T_i} \right]} = u_{m,max}^{(E)} . \tag{33}$$

The gas speed becomes zero when the temperature reaches its highest possible value, which, according to Eq. (29), is

$$T_{m,max}^{(E)} = \frac{\left(u_{m,max}^{(E)} \right)^2}{2R_m \sum_{i=0}^{n} \eta_i \left(\frac{H-E_o}{\mathcal{R}T} \right)_i^{T_m}} . \tag{34}$$

The relationship between temperature, T_m, and speed, u_m, according to the energy equation can now be written in the simple form

$$u_m^{(E)} = \sqrt{\left[u_{m,max}^{(E)} \right]^2 - 2R_m T_m \sum_{i=0}^{n} \eta_i \left(\frac{H-E_o}{\mathcal{R}T} \right)_i^{T_m}} . \tag{35}$$

According to this equation the speed of the mixture decreases steadily as the temperature is increased from $T_m = 0$ to its maximum value as given by Eq. (34).

For the case of a simple tangential ($\alpha_i = 0$) injection of hydrogen into a flow of oxygen the $u_m^{(E)}$ versus T_m [Eq. (35)] relationship, together with the $u_m^{(M-C)}$ versus T_m [Eq. (18)] relationship, are depicted in Fig. 10 for two different injection speeds (u_{H_2} = 200 m/s and u_{H_2} = 700 m/s). Since the actual flow of the gas mixture must satisfy all three fundamental equations {namely, continuity, momentum [Eqs. (17) or (18)], and energy [Eq. (35)]} only those points common to both curves represent possible conditions of the flow of the gas mixture.

Figure 10 reveals that there are 4 possibilities; i.e.,

(1) the two curves do not intersect at all as in the case for which u_{H_2} = 700 m/s,

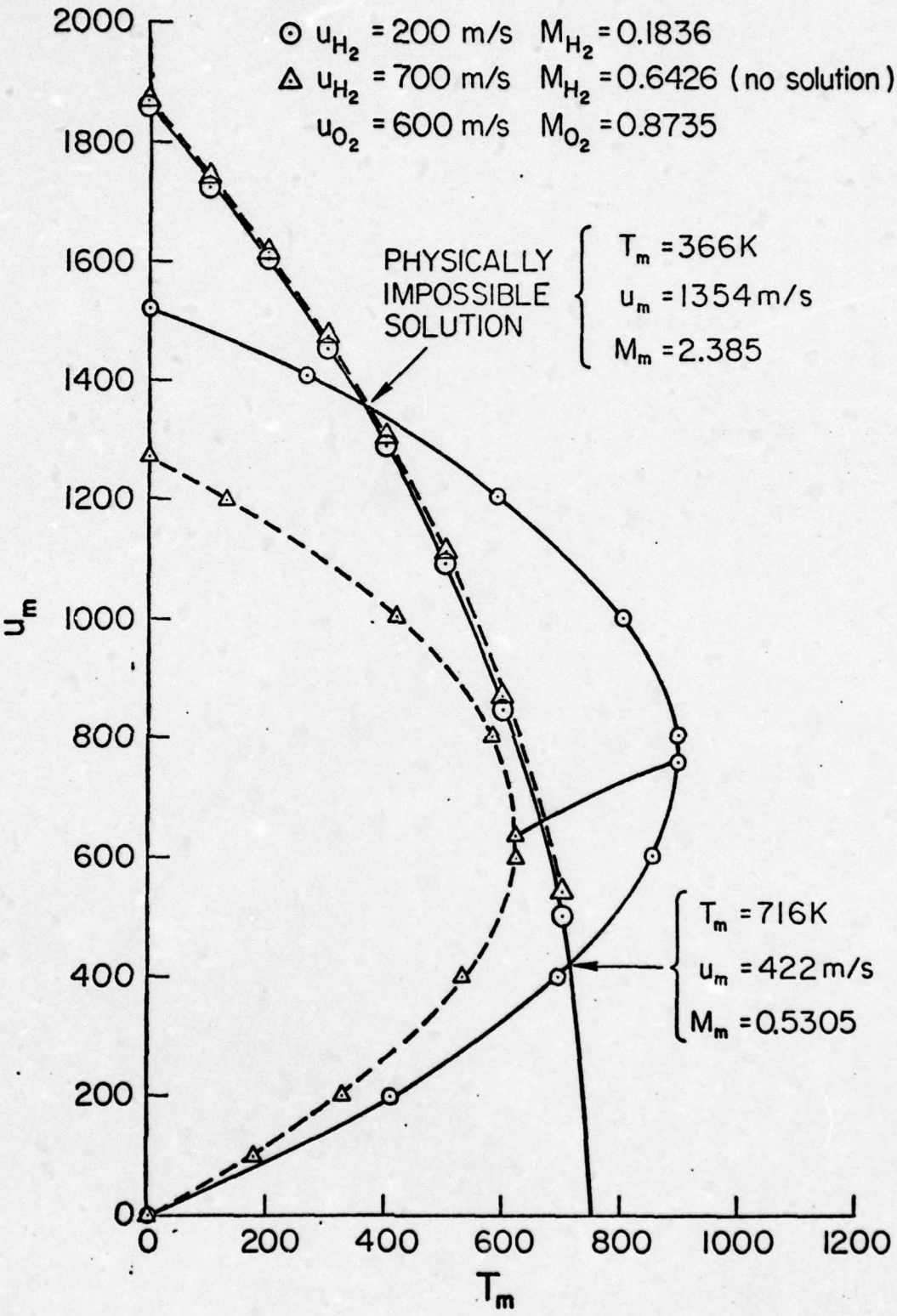

Fig. 10 - Relationships between final temperature, T_m, and gas speed, u_m, of mixture (subsonic flow)

(2) the $u_m^{(E)}$ versus T_m curve is tangent to the $u_m^{(M-C)}$ versus T_m curve (u_{H_2} = 492.5 m/s),

(3) the two curves intersect at two points (u_{H_2} = 200 m/s), and

(4) the two curves intersect only at one point ($u_{m,max}^{(E)} < u_{m,max}^{(M-C)}$).

When the two curves have no point in common, there is no solution because the mixing of the flows leads to choking. In other words the mixture cannot pass through the channel without proper adjustment of the initial conditions.

When the two curves have only the point in common where they are tangent to each other (possibility No. 2), the Mach number of the mixture is one (see Example No. 1). The point of tangency occurs always at a temperature which is slightly less than $T_{m,max}^{(M-X)}$ and at a speed which is somewhat greater than $1/2\, u_{m,max}$. For the case that the final gas temperature is equal to $T_{m,max}^{(M-C)}$ the Mach number of the flow is less than one, as the following calculation shows:

$$M_m^{T_{m,max}^{(M-C)}} = \frac{\frac{1}{2} u_{m,max}^{(M-C)}}{\sqrt{\gamma_m R_m T_{m,max}^{(M-C)}}} = \frac{\frac{1}{2} u_{m,max}^{(M-C)}}{\sqrt{\gamma_m R_m \frac{\left(0.5\, u_{m,max}^{(M-C)}\right)^2}{R_m}}} = \frac{1}{\sqrt{\gamma_m}} \qquad (36)$$

where the value for $T_{m,max}^{(M-C)}$ as given by Eq. (31) has been used. The point of tangency may be considered as the critical point since it is the limiting point of unchoked flow. Choking would occur at once when the speed of one of the two gases is increased slightly. The condition of choking can also be produced or relieved readily by variations of the temperatures, injection speeds, mole fractions of the constituents, and injection angle. It is obvious that the choking condition is more quickly produced with normal injection because of the constant area condition (see Example No. 3).

When the two curves have two points in common, there seem to be two different final flows for a given mixing process. For initially subsonic flows the solution with the higher temperature T_m and lower speed u_m (see Fig. 10) represents a subsonic flow ($M_m < 1$), whereas the solution with the lower temperature T_m but higher speed u_m represents a supersonic flow ($M_m > 1$). To determine whether both solutions represent physically possible processes it is necessary to calculate the entropy changes resulting from these processes. These calculations reveal that steady subsonic flows cannot be made supersonic by mixing because this transition involves a spontaneous decrease in entropy. Such a process could be accomplished only by an expansion shock wave which is physically impossible. On the other hand an initially supersonic flow may remain supersonic or it may become subsonic by experiencing a normal shock transition (see Example No. 2).

When the initial speeds are low or, more generally speaking, when the ordered motion kinetic energy and momentum are negligible in comparison with those of the random motion, the maximum possible speed from the momentum equation [Eq. (30)] becomes larger than that derived from the energy equation [Eq. (33)] and consequently the two curves have only one point in common in the positive coordinate quadrant. In this case only the subsonic solution exists; the second solution (supersonic; expansion shock!) involves a negative temperature.

In many respects the $u_m^{(E)}$ - T_m and $u_m^{(M-C)}$ - T_m curves may be considered as the counterparts of the Rayleigh and Hugoniot curves (in the p-v plane) for constant area duct flows with heat exchange or the Fanno curves for constant area duct flows subjected to viscous interaction at the duct walls. However, it is impossible to state how the various points of the u_m - T_m curves can be obtained by a certain mixing process because of the large number of initial parameters (u_i, T_i, x_i, m_i, and α_i) whereas Rayleigh, Hugoniot, and Fanno curves result from the variation of a single parameter (heat exchange or friction). Therefore, any change of any of the parameters of the initial gas (x_i, u_i, T_i, m_i) changes both the $u_m^{(E)}$ - T_m and the $u_m^{(M-C)}$ - T_m curve (see Fig. 10) whereas a change of q does not affect the Rayleigh line.

According to the previous discussions it is obvious that the temperature T_m and speed u_m of the gas mixture can be calculated by means of several different iteration procedures. The basic problem consists in finding a solution for two variables which appear in two equations which must be satisfied simultaneously but cannot be combined readily because of the complicated mathematical relationships between these two variables.

The solution requiring the lowest number of iterations is based on the fact that a rather reasonable value of the gas speed, u_m can be calculated when it is assumed that the term $\sum_{i=0}^{n} \eta_i \left(\frac{H-E_0}{\mathcal{R}T}\right)_i^{T_m} \equiv \sum$ changes only slightly with temperature and that the temperature of the mixture, T_m, cannot exceed the lower of the maxima given by Eqs. (30) and (33). Substitution of $T_m^{(M-C)}$ from Eq. (17) into Eq. (35) leads to a quadratic equation in u_m with the solution

$$u_m = u_{m,max}^{(M-C)} \cdot \frac{\Sigma}{2\Sigma-1} \left[1 \pm \sqrt{1 - \left(\frac{u_{m,max}^{(E)}}{u_{m,max}^{(M-C)}} \right)^2 \frac{2\Sigma-1}{\Sigma^2}} \right], \qquad (37)$$

where

$$\Sigma = \sum_{i=0}^{n} \eta_i \left(\frac{H-E_0}{\mathcal{R}T}\right)_i^{T_m} . \qquad (38)$$

For subsonic flows the positive sign in front of the radicand leads to the physically impossible expansion shock wave. Furthermore, we note that Eq. (37) has real solutions only when

$$\left(\frac{u_{m,max}^{(E)}}{u_{m,max}^{(M-C)}}\right)^2 \leq \frac{\Sigma^2}{2\Sigma-1} \cdot \tag{39}$$

This condition may serve as a simple criterion to determine whether choking occurs or not. For a quick answer to this question Fig. 11 was prepared. It depicts the dimensionless speed $\frac{u_m}{u_{m,max}^{(M-C)}}$ as a function of $\left(\frac{u_{m,max}^{(E)}}{u_{m,max}^{(M-C)}}\right)^2$ for various values of Σ. For a calorically perfect gas Σ is independent of temperature and no iteration is required. When Σ depends on temperature, the accuracy of the gas speed calculated by means of Eq. (37) depends on the accuracy of the estimated temperature and the rate at which Σ depends on temperature. With the fairly close approximation to the correct gas speed of the mixture, as given by Eq. (37), the temperature, as given by the momentum equation [Eq. (17)], is calculated. This temperature is now used as the starting point of the iteration procedure by calculating the difference $u_m^{(E)} - u_m^{(M-C)} = \Delta u_m$ by means of Eq. (35) and Eq. (18). For subsonic flows and for all $u_m < 1/2\ u_{m,max}^{(M-C)}$ this difference is positive when the temperature is less than the correct value and vice versa. For subsonic flows and $u_m > 1/2\ u_{m,max}^{(M-C)}$ this difference is positive when the temperature, used for calculating this difference, is greater than the correct value and vice versa (see Fig. 10 and Table 6). The calculations are repeated with properly adjusted temperatures $T_m^{(m)}$, until

$$\left|u_m^{(E)} - u_m^{(M-C)}\right| \leq \epsilon \ ,$$

where ϵ is a small number which should not be smaller than warranted by the accuracy of the thermodynamic functions used in these calculations.

After the correct values of the final gas speed, u_m, and temperature, T_m, have been determined, the static pressure of the gas mixture, p_m, can be calculated by means of Eq. (5) from which the channel cross-sectional area, A_m, is removed by the following relationships:

$$A_m = A_o + \sum_{i=1}^{n} A_i \cos\alpha_i \ ,$$

$$A_o = \dot{m}_o \frac{\mathcal{R}T_o}{p_o \mathcal{M}_o u_o} \ , \text{ and}$$

$$A_i = \dot{m}_i \frac{\mathcal{R}T_i}{p_i \mathcal{M}_i u_i} \ ,$$

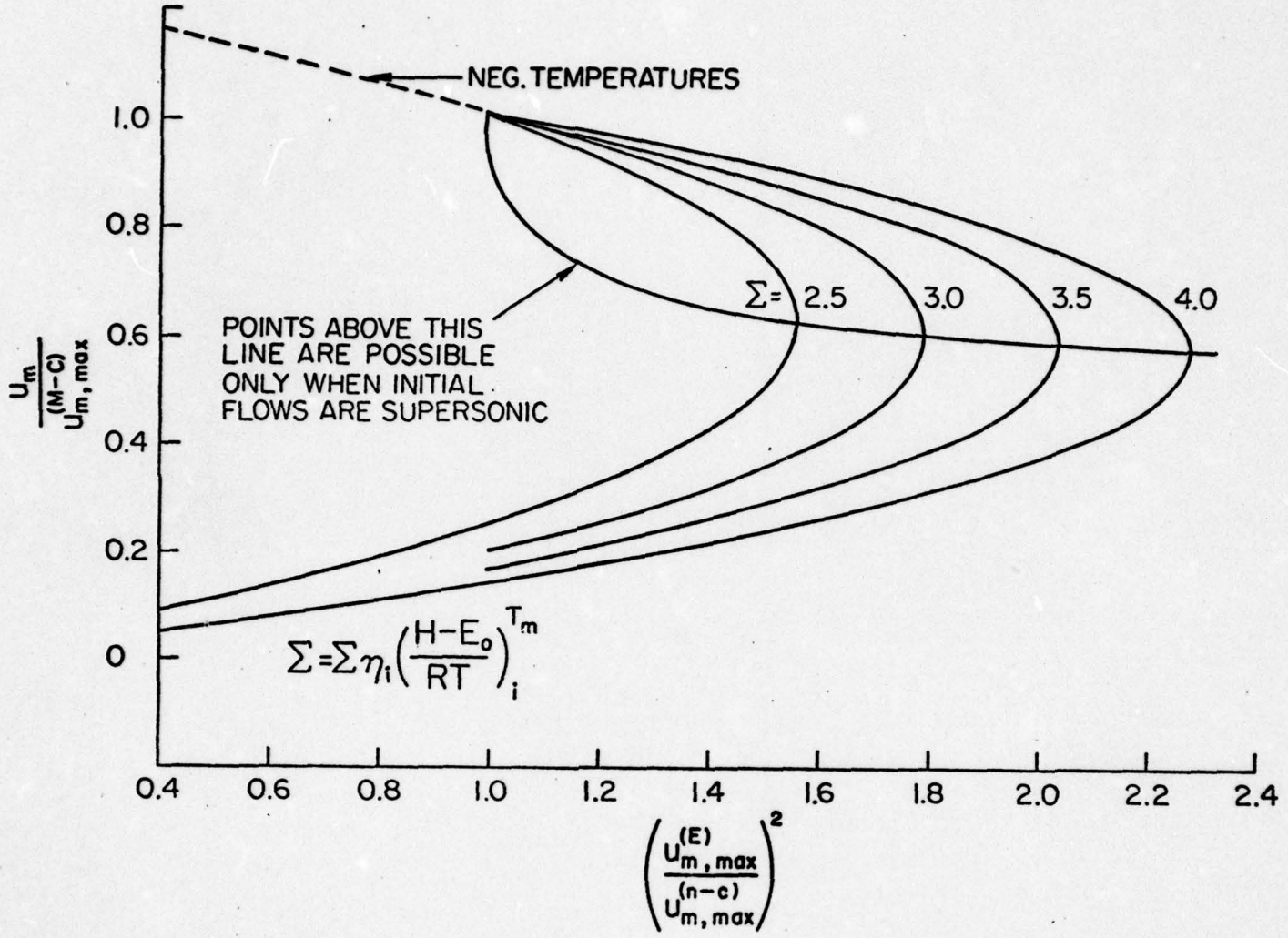

Fig. 11 - Dimensionless gas speed of mixture as a function of maximum gas speeds ratio

Table 6. Iteration for calculation of T_m and u_m

(a) u_{H_2} = 492 m/s

with $T_m^{(EST)}$ = 650 K we obtain from Eq. (37) $u_m^{(1)}$ = 736.8 m/s;
with $T_m^{(EST)}$ = 640 K we obtain from Eq. (37) $u_m^{(1)}$ = 745 m/s.
Then from Eq. (17): $T_m^{(1)} = T_m^{(M-C)} = \frac{u_m^{(1)} (1303.8 - u_m^{(1)})}{R_m}$ = 643 K and 641 K, respectively.

n	$T_m^{(n)}$	$u_m^{(M-C)}$	$u_m^{(E)}$	$\Delta u^{(n)}$	
1	643	737.47	738.30	0.83	
2	642	741.18	741.52	0.34	
3	641	744.75	744.73	-0.02	←subsonic solution
4	640	748.19	747.92	-0.27	
5	639	751.50	751.10	-0.40	
6	638	754.71	754,26	-0.45	
7	637	757.82	757.41	-0.41	
8	636	760.85	760.55	-0.30	
9	635	763.79	763.67	-0.12	
10	634	766.65	766.78	0.13	←supersonic solution

Subsonic Solution: T_m = 641.05 K, u_m = 744.56 m/s, M_m = 0.9840
Supersonic Solution: T_m = 634.48 K, u_m = 765.24 m/s, M_m = 1.0164

Table 6. (Continued)

(b) u_{H_2} = 100 m/s

with $T_m^{(EST)}$ = 700 K we obtain from Eq. (37) $u_m^{(1)}$ = 292.3 m/s.

Then from Eq. (17) $T_m^{(1)}$ = 735.7 K

n	$T_m^{(n)}$ (K)	$u_m^{(M-C)}$ (m/s)	$u_m^{(E)}$ (m/s)	$\Delta u^{(n)}$ (m/s)
1	735	291.990	284.266	-7.724
2	734	291.507	292.628	1.121
3	734.125	291.567	291.596	0.029

Solution: T_m = 734.13 K, u_m = 291.58 m/s, M_m = 0.3611

---

so that

$$p_m = \frac{\dot{m}}{\dot{m}_o \frac{\mathcal{R}T_o}{p_o \mathcal{M}_o u_o} + \sum_{i=1}^{n} \dot{m}_i \frac{\mathcal{R}T_i}{p_i \mathcal{M}_i u_i} \cos\alpha_i} \cdot \frac{\mathcal{R}T_m}{\mathcal{M}_m u_m} \cdot \tag{40}$$

Upon division of numerator and denominator by $\dot{m}$ and cancellation of $\mathcal{R}$ we arrive at

$$p_m = \frac{1}{\frac{x_o T_o}{p_o \mathcal{M}_o u_o} + \sum_{i=1}^{n} \frac{x_i T_i}{p_i \mathcal{M}_i u_i} \cdot \cos\alpha_i} \cdot \frac{T_m}{\mathcal{M}_m \cdot u_m} \cdot \tag{41}$$

According to Eq. (28) we have

$$\frac{x_i}{\mathcal{M}_i} = \frac{\eta_i}{\mathcal{M}_m} \cdot$$

Substitution of this relationship into Eq. (41) leads to

$$p_m = \frac{T_m}{u_m \left[\frac{\eta_o T_o}{p_o u_o} + \sum_{i=1}^{n} \frac{\eta_i T_i}{p_i u_i} \cos\alpha_i \right]} \cdot \qquad (42)$$

The ratio of the duct area through which the final flow of the mixture ($\dot{m}, A_m$) passes to that through which only the primary flow ($\dot{m}_o, A_o$) passes can be calculated as follows:

from $$A_m = A_o + \sum_{i=1}^{n} A_i \cos\alpha_i \ ,$$

with $$A_o = \frac{\dot{m}_o \mathcal{R} T_o}{p_o u_o \mathcal{M}_o}$$

and $$A_i = \frac{m_i \mathcal{R} T_i}{p_i u_i \mathcal{M}_i} \ ,$$

we obtain

$$\frac{A_m}{A_o} = 1 + \sum_{i=1}^{n} \frac{\dot{m}_i}{\dot{m}_o} \cdot \frac{T_i}{T_o} \cdot \frac{p_o}{p_i} \cdot \frac{u_o}{u_i} \cdot \frac{\mathcal{M}_o}{\mathcal{M}_i} \cos\alpha_i \ .$$

With $\dot{m}_i = \dot{m} \cdot x_i$ and $x_i = \eta_i \ (\mathcal{M}_i / \mathcal{M}_m)$

we arrive at

$$\frac{A_m}{A_o} = 1 + \sum_{i=1}^{n} \frac{\eta_i}{\eta_o} \cdot \frac{T_i}{T_o} \cdot \frac{p_o}{p_i} \cdot \frac{u_o}{u_i} \cdot \cos\alpha_i \ . \qquad (43)$$

The increase in entropy caused by the mixing of different gas flows follows from the expression for the entropy of gas mixtures. Before mixing we have

$$s = \sum_{i=0}^{n} x_i s_i \ , \qquad (44)$$

where

$$s_i = \frac{\mathcal{R}}{\mathcal{M}_i} \left[\left(\frac{S^{p=1}}{\mathcal{R}} \right)_i^{T_i} - \ln p_i \right] . \qquad (45)$$

After mixing we have

$$s_m = \frac{\mathcal{R}}{\mathcal{M}_m}\left[\sum_{i=0}^{n}\eta_i\left(\frac{S^{p=1}}{\mathcal{R}}\right)_i^{T_m} - \sum_{i=0}^{n}\eta_i \ln\eta_i - \ln p_m\right] \tag{46}$$

and thus

$$\frac{s_m - s}{R_m} = \sum_{i=0}^{n}\eta_i\left[\left(\frac{S^{p=1}}{\mathcal{R}}\right)_i^{T_m} - \left(\frac{S^{p=1}}{\mathcal{R}}\right)_i^{T_i}\right] - \sum_{i=0}^{n}\eta_i \ln\eta_i - \sum_{i=0}^{n}\eta_i \ln\frac{p_m}{p_i} . \tag{47}$$

2. Mixing of Gases at Rest

The previous equations can be used also to calculate the temperature resulting from the mixing of gases at rest ($u_o = 0$ and all $u_i = 0$). When the gases are not flowing, only the energy equation is available for calculating the final temperature T_m. When the pressure is held constant, Eq. (33) can be used. For $u_o = u_i = 0$ we obtain

$$u_{m,max}^{(E)} = \sqrt{2\sum_{i=0}^{n} x_i R_i T_i \left(\frac{H-E_o}{\mathcal{R}T}\right)_i^{T_i}} . \tag{48}$$

Substitution of this expression into Eq. (34) leads to

$$T^{static,dp=0} = \frac{\sum_{i=0}^{n} x_i R_i T_i \left(\frac{H-E}{\mathcal{R}T}\right)_i^{T_o}}{R_m \sum \eta_i \left(\frac{H-E_o}{\mathcal{R}T}\right)_i^{T_m}} . \tag{49}$$

With

$$\frac{x_i}{\mathcal{M}_i} = \frac{\eta_i}{\mathcal{M}_m} ,$$

as given by Eq. (28), we obtain

$$T^{static,dp=0} = \frac{\sum_{i=0}^{n} \eta_i T_i \left(\frac{H-E_o}{\mathcal{R}T}\right)_i^{T_i}}{\sum_{i=0}^{n} \eta_i \left(\frac{H-E_o}{\mathcal{R}T}\right)_i^{T_m}} . \tag{50}$$

At constant volume the internal energies, E_i, instead of the enthalpies must be used. With $E = H - \mathcal{R}T$ we obtain

$$T^{\text{static},dv=0} = \frac{\sum_{i=0}^{n} \eta_i T_i \left(\frac{E-E_0}{\mathcal{R}T}\right)_i^{T_i}}{\sum_{i=0}^{n} \eta_i \left(\frac{E-E_0}{\mathcal{R}T}\right)_i^{T_m}} = \frac{\sum_{i=0}^{n} \eta_i T_i \left[\left(\frac{H-E_0}{\mathcal{R}T}\right)_i^{T_i} - 1\right]}{\sum_{i=0}^{n} \eta_i \left(\frac{H-E_0}{\mathcal{R}T}\right)^{T_m} - 1} . \quad (51)$$

3. Mixing of Gas Flows Involving Chemical Changes

When chemical reactions occur as the gases are mixed, the calculations become much more tedious. First of all the reduced sensible enthalpies in the energy equation must be replaced by the reduced formation enthalpies, $\left(\frac{\Delta H_f}{\mathcal{R}T}\right)_i^T$. Only the case that the final gas mixture is in a state of complete thermodynamic and chemical equilibrium will be discussed here. Since the composition of the reacting gas mixture depends not only on temperature but also on pressure, the calculations must be started with estimated values of the final temperature, T_c, and the final pressure, p_c. The subscript c is used to stress the fact that chemical reactions have been included and to distinguish this state from the non-reacting mixture for which the subscript m is being used.

With the estimated values of temperature, $T_c^{(1)}$, and pressure, $p_c^{(1)}$, the composition ($\eta_{i,c}$) of the final gas is calculated according to the standard procedure. Then, according to the energy equation [see Eq. (35)], the gas speed u_c, is calculated for this temperature and composition;

$$u_c^{(E)} = \sqrt{\left[u_{m,\text{limit}}^{(E)}\right]^2 - 2R_c T_c \Sigma \eta_{i,c} \left(\frac{\Delta H_f}{\mathcal{R}T}\right)_i^{T_c}} , \quad (52)$$

where

$$u_{m,\text{limit}}^{(E)} = \sqrt{\sum_{i=0}^{n} x_i \left[u_i^2 + 2R_i T_i \left(\frac{\Delta H_f}{\mathcal{R}T}\right)_i^{T_i}\right]} . \quad (53)$$

For exothermic chemical changes the speed $u_{m,\text{limit}}^{(E)}$ is no longer the largest possible value. At low temperatures the sum of the formation enthalpies at T_c in Eq. (52) may become negative. Therefore, the speed $u_{m,\text{limit}}^{(E)}$ is reached at a temperature where $\sum_{i=0}^{n} \eta_{i,c} \left(\frac{\Delta H_f}{\mathcal{R}T}\right)_i^{T_c}$ is equal to zero. For lower temperatures $u_m^{(E)}$ exceeds the so-called limiting value, $u_{m,\text{limit}}^{(E)}$. Whether these conditions represent physically possible solutions cannot be said in general. Since they can occur only in subsonic flows (these temperatures are lower than the constant pressure adiabatic flame temperatures) it may be expected that these low temperatures lead to the impossible expansion shock.

Since the calculations can be started only with an arbitrarily assumed pressure, the correct pressure must be established by iteration. According to the continuity equation the pressure must satisfy the condition [see Eq. (3)]

$$p_c = \frac{\dot{m}}{A_m} \cdot \frac{\mathcal{R}T_c}{u_c \cdot \mathcal{M}_c} , \tag{54}$$

where $\frac{\dot{m}}{A_m}$ is given by the thermodynamic and gasdynamic values of the initial flows before mixing. With

$$A_m = A_o + \sum_{i=1}^{n} A_i \cos\alpha_i$$

and

$$A_i = \frac{m_i}{p_i} \cdot \frac{\mathcal{R}T_i}{\mathcal{M}_i u_i}$$

we obtain

$$\frac{\dot{m}}{A_m} = \frac{\dot{m}}{\frac{m_o}{p_o} \cdot \frac{\mathcal{R}T_o}{\mathcal{M}_o u_o} + \sum_{n=1}^{n} \frac{m_i}{p_i} \cdot \frac{\mathcal{R}T_i}{\mathcal{M}_i u_i} \cdot \cos\alpha_i} . \tag{55}$$

Upon division of numerator and denominator by $\dot{m}$ and with Eq. (28) we arrive at

$$\frac{\dot{m}}{A_m} = \frac{1}{R_m \left[\frac{\eta_o T_o}{p_o u_o} + \sum_{i=1}^{n} \frac{\eta_i T_i}{p_i u_i} \cos\alpha_i \right]} , \tag{56}$$

where $\mathcal{M}_m = \sum_{i=0}^{n} \eta_{i,1} \mathcal{M}_i$ is the molecular mass of the unreacted mixture. Substitution of Eq. (56) into Eq. (54) leads to

$$p_c = \frac{\mathcal{M}_m T_c}{u_c \mathcal{M}_c \left[\frac{\eta_o T_o}{p_o u_o} + \sum_{i=1}^{n} \frac{\eta_i T_i}{p_i u_i} \cos\alpha_i \right]} . \tag{57}$$

Thus the pressure corresponding to the assumed temperature, $T_c^{(1)}$, is

$$p_{c,calc.}^{(1)} = \frac{\mathcal{M}_m T_c^{(1)}}{u_c^{(E)} \mathcal{M}_c \left[\frac{\eta_o T_o}{p_o u_o} + \sum_{i=1}^{n} \frac{\eta_i T_i}{p_i u_i} \cos\alpha_i \right]} \cdot \qquad (58)$$

For the selected temperature ($T_c^{(1)}$) of the chemically reacting gas mixture an increase in pressure reduces the amount of dissociation as long as at least one of the mole number changes, $\Delta\nu^{(j)}$, of the σ chemical changes occurring in the mixture is not zero. On the other hand a decrease in pressure increases the amount of dissociation in this case. Because of this effect the molecular mass, $\mathcal{M}_c = \sum_{i=1}^{z} \eta_{i,c} \mathcal{M}_i$ (z = number of species in equilibrium mixture), and the speed, $u_c^{(E)}$, will increase as the pressure is increased and vice versa. Consequently, the pressure calculated by means of Eq. (58) will decrease when a higher value is used for the estimated pressure. Therefore, a new estimate, $p_{c,est}^{(n)}$, can be obtained as a simple average of the calculated and estimated values;

$$p_{c,est}^{(n)} = \left(p_{c,calc}^{(n-1)} + p_{c,est}^{(n-1)} \right) \cdot 0.5 \, . \qquad (59)$$

When the composition of the reacting gas mixture is not affected very much by pressure variations, the iteration formula [Eq. (59)] may be replaced by the expression

$$p_{c,est}^{(n)} = p_{c,calc}^{(n-1)} + \left[p_{c,est}^{(n-1)} - p_{c,calc}^{(n-1)} \right] \cdot x \, , \qquad (60)$$

where x is an empirical factor between 0 and 0.5. The iterations are continued until the difference between calculated and estimated pressure satisfies the condition

$$\left| p_{c,calc}^{(n)} - p_{c,est}^{(n)} \right| \leq \epsilon \, , \qquad (61)$$

where ϵ is a small number in accordance with the desired accuracy. After the correct pressure, p_c, has been determined it is necessary to check the validity of the temperature estimate, $T_c^{(1)}$. To perform this test both gas speeds, $u_c^{(E)}$ and $u_c^{(M-C)}$, are calculated with this temperature estimate, $T_c^{(1)}$, and the corresponding pressure, p_c, by means of Eq. (52) and Eq. (18), which now is written as

$$u_c^{(M-C)} = \frac{1}{2} u_{m,max}^{(M-C)} \pm \sqrt{\left[\frac{1}{2} u_{m,max}^{(M-C)} \right]^2 - R_c T_c} \, , \qquad (62)$$

where, as in the non-reacting case,

$$u_{m,max}^{(M-C)} = x_o u_o \left(1 + \frac{R_o T_o}{u_o^2}\right) + \sum_{i=1}^{n} x_i u_i \left(1 + \frac{R_i T_i}{u_i^2}\right) \cos\alpha_i \ .$$

However, the maximum temperature, $T_{c,max}^{(M-C)}$, must now be based on the molecular mass of the mixture of the products formed by the chemical changes at this temperature. Therefore, instead of Eq. (31) we have for the reacting mixture

$$T_{c,max}^{(M-C)} = \frac{\left[0.5 u_{m,max}^{(M-C)}\right]^2}{\mathcal{R}} \cdot \mathcal{M}_{T_{c,max}^{(M-C)}} \ . \qquad (63)$$

Because of this relationship the temperature, $T_{c,max}^{(M-C)}$, can only be estimated. Actually a rigorous value is not needed. However this temperature limit may be of some help in establishing the first estimate, $T_c^{(1)}$, which must be lower than this limit although it is not possible to state how much lower it should be. If $\Delta u_c^{(n)} = u_c^{(E)} - u_c^{(M-C)} \neq 0$, the calculations have to be repeated with $T_c^{(n+1)} > T_c^{(n)}$, when $\Delta u_c^{(n)} > 0$ for subsonic flow and $u_c < 1/2\ u_{c,max}^{(M-C)}$, whereas $T_c^{(n+1)} < T_c^{(n)}$ when $\Delta u_c^{(n)} > 0$ for subsonic flow and $u_c > 1/2\ u_{c,max}^{(M-C)}$. When $\Delta u_c^{(n)} < 0$, the opposite changes in temperature must be made. For supersonic flows, positive values of $\Delta u_c^{(n)}$ indicate that the temperature estimate, $T_c^{(n)}$, was too low and vice versa. The iterations are continued until $\left|\Delta u_c^{(n)}\right| \leq \epsilon$ where ϵ is again a properly chosen small value.

To illustrate these techniques let us consider the flow of oxygen (primary flow) to which hydrogen is added at various conditions (Example No. 1).

Approximate values of the final speed of the gas mixture, $u_m^{(1)}$, as calculated from Eq. (37) with estimated temperatures obtained from Table 7, are compiled in Table 9 together with the rigorous calculations of T_m, u_m, p_m, M_m, $\frac{Am}{A_{O_2}}$, and the increase in entropy, $\frac{\Delta s}{R_m}$. This table reveals that approximate values of the gas speeds deviate in most cases by less than 1% from the exact values. The estimated temperatures, of course, are less reliable. Table 10 a and b have been included to show the rate of convergence of the iterations leading to the correct values of u_m for $u_{H_2} = 492$ (m/s) and $u_{H_2} = 100$ (m/s), respectively. For $u_{H_2} = 492$ (m/s) the iteration producing the supersonic solution (impossible expansion shock) has been included in order to show that this injection speed produces two solutions which are very close to the critical conditions ($M_m = 1$) at which the flow becomes choked. For $u_{H_2} = 493$ (m/s)

EXAMPLE 1

A subsonic flow of hydrogen is injected tangentially into a subsonic flow of oxygen.

The initial conditions of the oxygen flow are:

T_{O_2} = 1400 K

M_{O_2} = 0.8735

u_{O_2} = 600 m/s

p_{O_2} = 1 atm

η_{O_2} = 0.36 (x_{O_2} = 0.9) $\mathcal{M}_{O_2}$ = 32 kg/kmol

The initial conditions of the various hydrogen flows are:

T_{H_2} = 200 K (for all speeds u_{H_2})

u_{H_2} =	100 m/s	M_{H_2} = 0.0918
=	200 m/s	= 0.1836
=	400 m/s	= 0.3672
=	450 m/s	= 0.4131
=	490 m/s	= 0.4498
=	492 m/s	= 0.4517

p_{H_2} = 1 atm

η_{H_2} = 0.64 (x_{H_2} = 0.1) $\mathcal{M}_{H_2}$ = 2 kg/kmol

The values of $u_{m,max}^{(M-C)}$, $T_{m,max}^{(M-C)}$, $u_{m,max}^{(E)}$, $T_{m,max}^{(E)}$, and $\left(\frac{u_{m,max}^{(E)}}{u_{m,max}^{(M-C)}}\right)^2$ for the seven different hydrogen injection speeds, u_{H_2}, are listed in Table 7. For the temperatures, which the final flows are estimated to attain, the values of $\sum = \sum \eta_{i,1} \cdot \left(\frac{H-E_0}{\mathcal{R}T}\right)_i^T$ and the functions of Σ appearing in Eq. (37) are compiled in Table 8.

Table 7. Parameters for calculating flow mixing

u_{H_2}	$u_{m,max}^{(M-C)}$	$T_{m,max}^{(M-C)}$	$u_{m,max}^{(E)}$	$T_{m,max}^{(E)}$	$\left(\frac{u_{m,max}^{(E)}}{u_{m,max}^{(M-C)}}\right)^2$
100	1927.1	1429.3	1860.9	749	0.9325
200	1521.3	890.8	1861.7	750	1.4974
400	1333.5	684.4	1864.8	753	1.9958
450	1315.4	665.9	1866.0	754	2.0124
490	1304.3	654.8	1867.0	755	2.0489
492	1303.8	654.3	1867.1	755	2.0506
700	1274.4	625.1	1873.7	760	2.1618

Table 8. Reduced sensible enthalpy of initial gases

T (K)	$\Sigma \equiv \Sigma n_i \cdot \left(\frac{H-E_0}{\Re T}\right)_i$	$\frac{\Sigma^2}{2\cdot\Sigma - 1}$	$\frac{\Sigma}{2\cdot\Sigma - 1}$
500	3.4884	2.0358	0.5837
600	3.5108	2.0469	0.5830
640	3.5200	2.0514	0.5828
650	3.5223	2.0526	0.5827
660	3.5246	2.0535	0.5827
680	3.5292	2.0558	0.5825
700	3.5338	2.0581	0.5824
750	3.5454	2.0638	0.5821

Table 9. Final state of flowing mixture

u_{H_2} (m/s)	$T_m^{(EST)}$ (K)	$u_m^{(1)}$ (m/s)	T_m (K)	u_m (m/s)	p_m (atm)	M_m	$\frac{A_m}{A_{O_2}}$	$\frac{s_m - s}{R_m}$
100	700	292.3	734.13	291.58	1.1876	0.3611	2.5238	2.3925
200	700	423.6	715.26	423.00	1.1425	0.5302	1.7619	2.3376
400	660	607.6	678.63	605.58	0.9661	0.7785	1.3810	2.3086
450	650	659.2	665.94*	657.02	0.9014	0.8531	1.3386	2.3061
490	650	727.6	645.00	731.73	0.8004	0.9642	1.3110	2.3063
492	650	736.8	641.05	744.56	0.7826	0.9840	1.3097	2.3065

*Note: This temperature is equal to $T_{m_1}^{(M-C)}{}_{max}$ as given in Table 7 for u_{H_2} = 450 m/s

Table 10. Iteration for calculation of T_m and u_m

(a) u_{H_2} = 492 m/s ;

with $T_m^{(EST)}$ = 650 K we obtain from Eq. (37),

$u_m^{(1)}$ = 736.8 m/s ;

with $T_m^{(EST)}$ = 640 K we obtain from Eq. (37) $u_m^{(1)}$ = 745 m/s

Then from Eq. (17): $T_m^{(1)} = T_m^{(M-C)} = \frac{u_m^{(1)}\left(1303.8 - u_m^{(1)}\right)}{R_m}$ = 643 K and 641 K, respectively.

n	$T_m^{(n)}$ (K)	$u_m^{(M-C)}$ (m/s)	$u_m^{(E)}$ (m/s)	$\Delta u^{(n)}$ (m/s)	
1	643	737.47	738.30	0.83	
2	642	741.18	741.52	0.34	←subsonic solution
3	641	744.75	744.73	-0.02	
4	640	748.19	747.92	-0.27	
5	639	751.50	751.10	-0.40	
6	638	754.71	754.26	-0.45	
7	637	757.82	757.41	-0.41	
8	636	760.85	760.55	-0.30	
9	635	763.79	763.67	-0.12	
10	634	766.65	766.78	0.13	←supersonic solution

Subsonic Solution: T_m = 641.05 K, u_m = 744.56 m/s, M_m = 0.9840

Supersonic Solution: T_m = 634.48 K, u_m = 765.24 m/s, M_m = 1.0164

Table 10. (continued)

(b) u_{H_2} = 100 m/s ;

with $T_m^{(EST)}$ = 700 K we obtain from Eq. (37), $u_m^{(1)}$ = 292.3 m/s ;

Then from Eq. (17): $T_m^{(1)}$ = 735.7 K

n	$T_m^{(n)}$ (K)	$u_m^{(M-C)}$ (m/s)	$u_m^{(E)}$ (m/s)	$\Delta u^{(n)}$ (m/s)
1	735	291.990	284.266	-7.724
2	734	291.507	292.628	1.121
3	734.125	291.567	291.596	0.029

Solution: T_m = 734.13 K, u_m = 291.58 m/s, M_m = 0.3611

---

there is no solution. Hence, choking begins at injection speeds between 492 and 493 m/s. Because of the large number of initial parameters of the flows it is not possible to prove analytically that at the point of choking the two curves become tangent to each other. However, a graphical presentation of the conditions near choking in the u_m - T_m plane shows that the condition of tangency exists at M_m = 1. At the point where the temperature $T_m^{(M-C)}$ reaches its maximum (u_{H_2} = 450 m/s) we have $M_m = \frac{1}{\sqrt{7}}$ (see Table 9). The effect of the hydrogen injection speed, u_{H_2}, on the final state of the mixture is shown in Fig. 12.

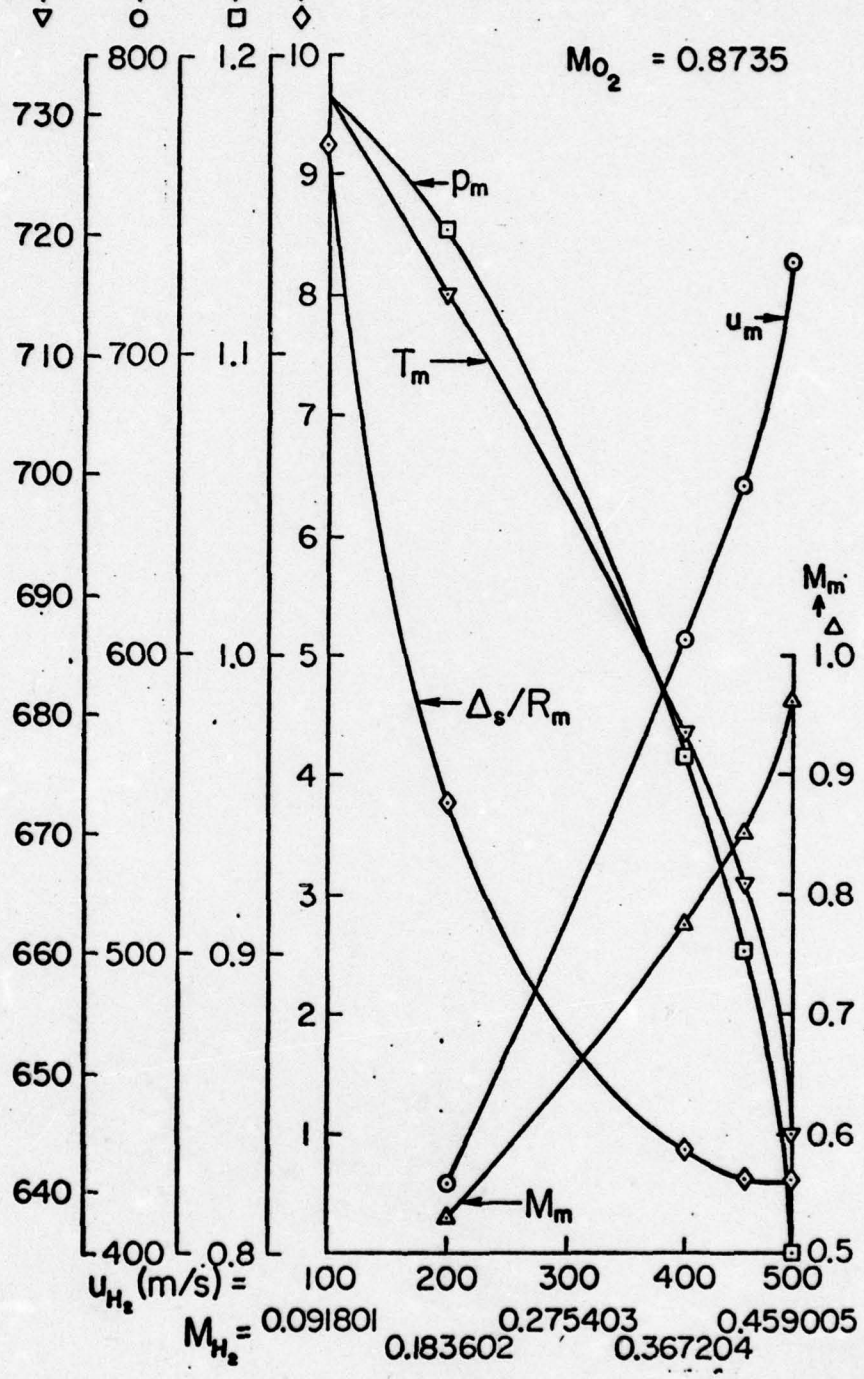

Fig. 12 - Effect of injection speed (α_{H_2} = 0) on final state of mixture (Example 1)

EXAMPLE 2

A supersonic flow of hydrogen is injected tangentially into a supersonic flow of oxygen. The initial conditions are:

$u_{H_2} = 2000$ m/s $\qquad u_{O_2} = 1400$ m/s

$T_{H_2} = 200$ K $\qquad T_{O_2} = 1000$ K

$p_{H_2} = 1$ atm $\qquad p_{O_2} = 1$ atm

$M_{H_2} = 1.8287$ $\qquad M_{O_2} = 2.3969$

$\eta_{H_2} = 0.64$ $\qquad \eta_{O_2} = 0.36$

For these conditions we have

$$u_{m,max}^{(M-C)} = \sum_{i=0}^{1} x_i u_i \left(1 + \frac{R_i T_i}{u_i^2}\right) = 1668.60 \text{ m/s} ,$$

$$u_{m,max}^{(E)} = \sqrt{\sum_{i=0}^{1} x_i \left[u_i^2 + 2R_i T_i \left(\frac{H-E_o}{\mathcal{R}T}\right)_i^{T_i}\right]} = 2121.17 \text{ m/s} ,$$

$$T_{m,max}^{(M-C)} = \frac{\left(0.5 u_{m,max}^{(M-C)}\right)^2}{R_m} = 1071.59 \text{ K} ,$$

$$T_{m,max}^{(E)} = \frac{\left(u_{m,max}^{(E)}\right)^2}{2R_m \sum_{i=0}^{1} \eta_i \left(\frac{H-E_o}{\mathcal{R}T}\right)_i^{T_m}} \simeq 962 \text{ K, and}$$

$$\left(\frac{u_{m,max}^{(E)}}{u_{m,max}^{(M-C)}}\right)^2 = 1.6160 .$$

According to Fig. 11 solutions exist since $\Sigma > 3.5$. Assuming $T_m = 600$ K ($\Sigma = 3.5108$) for the supersonic solution, we obtain from Eq. (37) (+ sign),

$$u_m^{(1)} = 1419 \text{ m/s} .$$

With this value the first temperature estimate according to Eq. (17) is

$$T_m^{(1)} = 545 \text{ K} .$$

Iteration leads to $u_m = 1417.72$ m/s and $T_m = 547.63$ K, $M_m = 2.0224$ so that according to Eq. (57) $p_m = 1.202814$ atm. Assuming $T_m = 900$ K ($\Sigma = 3.5803$) for the subsonic solution we obtain from Eq. (37) (- sign),

$$u_m^{(1)} = 511 \text{ m/s} .$$

With this value the first temperature estimate according to Eq. (17) becomes

$$T_m^{(1)} = 911 \text{ K} .$$

Iteration leads to $u_m = 510.91$ m/s and $T_m = 910.58$ K so that $M_m = 0.5701$ and $p_m = 5.549776$ atm.

The ratio of the pressures of the two solutions is

$$\frac{p_m^{(M_m<1)}}{p_m^{(M_m>1)}} = 4.613994 .$$

According to the normal shock relationships for a gas with variable specific heats we have

$$\left(\frac{p_2}{p_1}\right)_{N.S.} = \left(\frac{T_2}{T_1}\right)_{N.S.} \cdot \left(\Sigma^{T_2} - 0.5\right) - \left(\Sigma^{T_1} - 0.5\right) + \sqrt{\left\{\left(\frac{T_2}{T_1}\right)_{N.S.} \left(\Sigma^{T_2} - 0.5\right) - \left(\Sigma^{T_1} - 0.5\right)\right\}^2 + \left(\frac{T_2}{T_1}\right)_{N.S.}} ,$$

where $\Sigma^T = \Sigma \eta_i \cdot \left(\frac{H-E_0}{\mathcal{R}T}\right)_i^T$.

With $T_2 = T_m^{(M_m<1)} = 910.58$ K and $T_1 = T_m^{(M_m>1)} = 547.63$ K ,

we have $\Sigma^{T_2} = 3.583$ and $\Sigma^{T_1} = 3.499$,

so that $\left(\frac{p_2}{p_1}\right)_{N.S.} = 4.614$,

which is an exact agreement with the ratio of the pressures of the two solutions;

$$\frac{p_m^{(M_m<1)}}{p_m^{(M_m>1)}} = 4.614$$

The curves of $u_m^{(M-C)}$ versus T_m and $u_m^{(E)}$ versus T_m are shown in Fig. 13. Although these curves represent relationships between the final

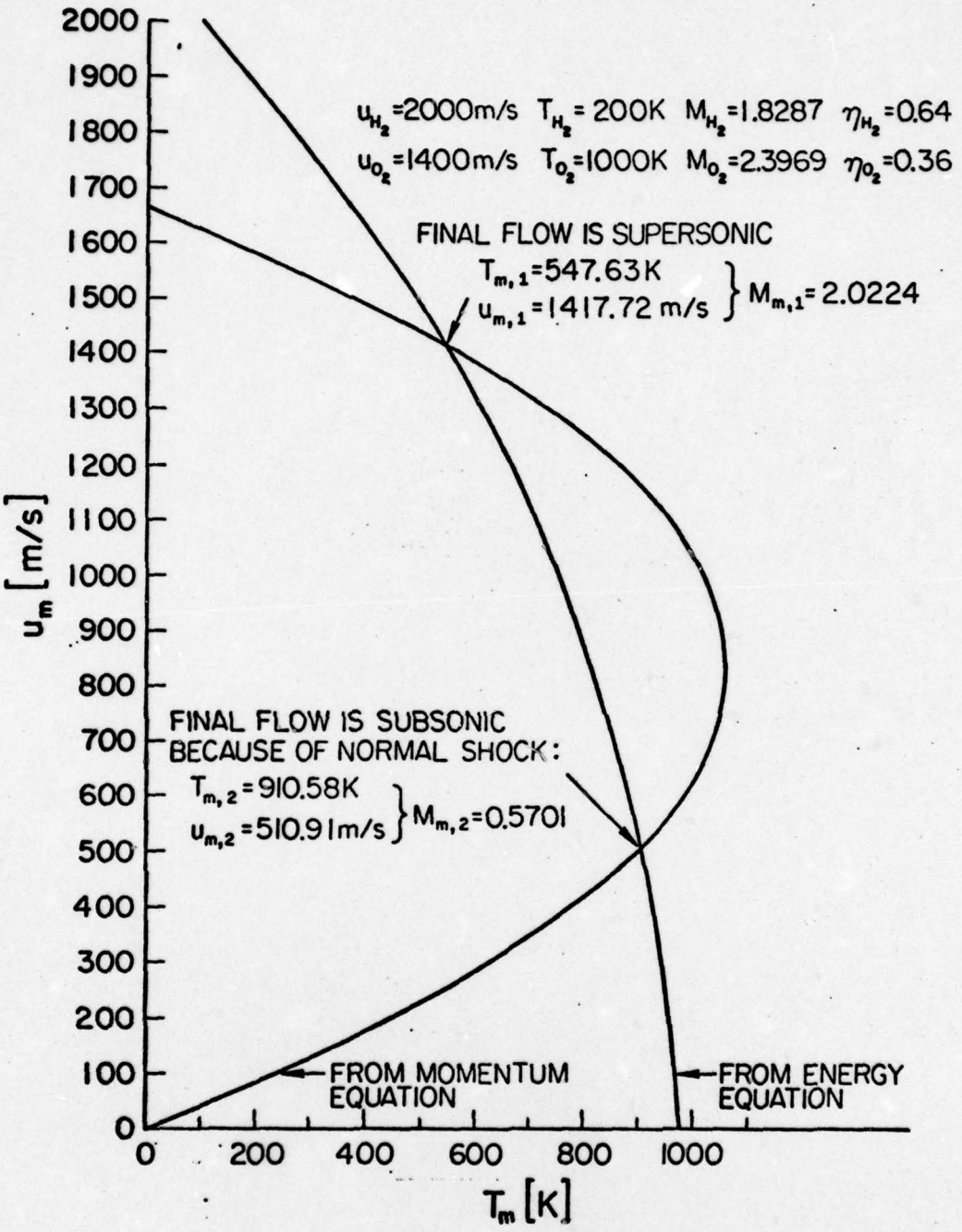

Fig. 13 - Relationships between final temperature, T_m, and gas speed, u_m, of mixture (initial flows are supersonic)

temperature and gas speed, only the points common to both curves are related to the initial conditions; all other points have no relationship to them. Also, because of the reduction in number of variables from T_i, p_i, u_i to T_m, p_m, u_m it is not possible to present graphically the path from the initial to the final conditions.

EXAMPLE 3

A subsonic flow of hydrogen is injected normally into a subsonic flow of oxygen. The initial conditions are

$u_{H_2} = 200$ m/s $\qquad u_{O_2} = 300$ m/s

$T_{H_2} = 200$ K $\qquad T_{O_2} = 1400$ K

$p_{H_2} = 1$ atm $\qquad p_{O_2} = 1$ atm

$M_{H_2} = 0.182872$ $\qquad M_{O_2} = 0.436736$

$\eta_{H_2} = 0.64$ $\qquad \eta_{O_2} = 0.36$

The linear speed of the primary flow (oxygen) in this example had to be much lower than that in the first example (tangential injection) in order to avoid choking even when the hydrogen is added at a very low speed.

With the initial conditions as given above we have

$$u_{m,max}^{(M-C)} = x_{O_2} \cdot u_{O_2} \cdot \left(1 + \frac{R_{O_2} T_{O_2}}{u_{O_2}^2}\right) = 1361.255812 \text{ m/s}$$

and

$$u_{m,max}^{(E)} = \sqrt{\sum_{i=0}^{1} x_i \left[u_i^2 + 2R_i T_i \left(\frac{H-E_o}{\mathcal{R}T}\right)_i^{T_i}\right]} = 1795.22 \text{ m/s} ,$$

and thus

$$\left(\frac{u_{m,max}^{(E)}}{u_{m,max}^{(M-C)}}\right)^2 = 1.7392 .$$

According to Fig. 11 this speed ratio is well below the critical value leading to choking when $\Sigma \geq 3.5$.

For the maximum temperature we obtain

$$T_{m,max}^{(M-C)} = 713.185023 \text{ K}$$

and

$$T_{m,max}^{(E)} = 702 \text{ K } (\Sigma = 3.53376 \text{ @ } 700 \text{ K}) .$$

In accordance with these values we use an estimated temperature of 600 K for which $\Sigma = 3.5108$ and thus from Eq. (37)

$$u_m^{(1)} = 485.95 \text{ m/s} ,$$

and according to Eq. (17)

$$T_m^{(1)} = 654.8 \text{ K} .$$

Iteration leads to

$$\left.\begin{aligned} T_m &= 653.16 \text{ K} \\ u_m &= 483.19 \text{ m/s} \end{aligned}\right\} M_m = 0.632804$$

and

$$p_m = \frac{T_m}{u_m \cdot \dfrac{\eta_{O_2} T_{O_2}}{p_{O_2} u_{O_2}}} = 0.804623 \text{ atm} .$$

An increase of the oxygen speed, u_{O_2}, from 300 to 400 m/s, reduces $u_{m,max}^{(M-C)}$ to 1178.44 m/s and increases $u_{m,max}^{(E)}$ to 1812.68 m/s, so that

$$\left(\frac{u_{m,max}^{(E)}}{u_{m,max}^{(M-C)}}\right)^2 = 2.366,$$

which, according to Fig. 11, means that the addition of hydrogen to this flow causes choking. On the other hand, an increase of the hydrogen speed, u_{H_2}, from 200 to 800 m/s, raises the final Mach number by 2.56% (from 0.6328 to 0.6490). The final conditions for this case are

$$\left.\begin{aligned} T_m &= 662.5 \text{ K} \\ u_m &= 499 \text{ m/s} \end{aligned}\right\} M_m = 0.6490$$

$$p_m = 0.7903 \text{ atm.}$$

EXAMPLE 4

A subsonic flow of hydrogen ($M_{H_2} = 0.0918$) is added tangentially to a subsonic flow of oxygen ($M_{O_2} = 0.2912$). Calculate the final state of the mixture after combustion has occurred and complete chemical equilibrium has been established.

Because of the high combustion enthalpy of hydrogen, choking occurs at the oxygen speeds, u_{O_2}, used in the previous examples. Using the criterion

$$\frac{q}{c_p T_m} \leq \frac{1}{2(\gamma+1)} \left(M_m - \frac{1}{M_m} \right)^2 , \tag{64}$$

which applies to constant area duct flows with heat addition, it was estimated that the following initial parameters would not lead to choking:

$u_{H_2} = 100$ m/s $\qquad u_{O_2} = 200$ m/s

$T_{H_2} = 200$ K $\qquad T_{O_2} = 1400$ K

$\eta_{H_2} = 0.64$ $\qquad \eta_{O_2} = 0.36$

The final state of the gas mixture was calculated by two methods:

(1) First the state of the mixture was calculated without consideration of any chemical changes according to the procedure explained in the previous examples. Starting then with these uniform conditions (denoted by the subscript m) the final state (denoted by the subscript c) was determined by finding for a constant area duct flow ($A_c = A_m$) the pressure and temperature ratios which satisfy simultaneously the Rayleigh line (momentum equation from which u_c has been removed by means of the continuity equation),

$$\frac{\frac{p_c}{p_m} - 1}{1 - \frac{v_c}{v_m}} \equiv (s.r.)^2 = \frac{u_m^2}{R_m T_m} , \tag{65}$$

and the Hugoniot curve (energy equation from which both speeds have been eliminated by means of the momentum and continuity equations),

$$\frac{h_f^{T_c} - h_f^{T_m}}{R_m T_m} = \frac{1}{2} \left(\frac{p_c}{p_m} - 1 \right) \left(1 + \frac{v_c}{v_m} \right) , \tag{66}$$

where

$$\frac{v_c}{v_m} = \frac{T_c}{T_m} \cdot \frac{p_m}{p_c} \cdot \frac{\mathcal{M}_m}{\mathcal{M}_c} \cdot \tag{67}$$

Both the Rayleigh and Hugoniot relationships contain only T_c and p_c as the unknown variables. However, an explicit solution cannot be established because of the complicated relationships between these variables and the formation enthalpies

$$\frac{h_f^T}{R_m T_m} = \frac{T}{T_m} \cdot \frac{\mathcal{M}_m}{\mathcal{M}} \sum_{i=0}^{2} \eta_i \left(\frac{\Delta H_f}{\mathcal{R}T}\right)_i^T \cdot \tag{68}$$

Therefore, the two equations (65 and 66) must be solved simultaneously by an iteration technique which has to be started not only with an estimated value of the final temperature, T_c, but also with an estimate of the final pressure, p_c.

With these estimates first the composition ($\eta_{i,c}$) of the final gas is calculated (see Worksheet No. 1). Using this composition we must determine whether the estimated pressure, together with the estimated temperature, satisfies the Hugoniot equation (66). This test is performed by determining a so-called calculated pressure from Eq. (66). In deriving the expression for the calculated pressure, $p_{c,calc}$, the effect of pressure on the formation enthalpy of the final gas mixture is ignored. Thus from Eq. (66) we obtain

$$p_{c,calc}^{(n)} = p_m \left\{ a + \sqrt{a^2 + \frac{T_{e,est}}{T_m} \cdot \frac{\mathcal{M}_m}{\mathcal{M}_c}} \right\}, \tag{69}$$

where

$$\mathcal{M}_c = \sum \eta_{i,c} \mathcal{M}_i$$

and

$$a = \frac{h_f^{T_c} - h_f^{T_m}}{R_m T_m} - 0.5 \cdot \left[\frac{T_{c,est}^{(n)}}{T_m} \cdot \frac{\mathcal{M}_m}{\mathcal{M}_c} - 1 \right]. \tag{70}$$

The superscript (n) denotes the nth estimate. If $p_{c,calc}^{(n)} \neq p_{c,est}^{(n)}$, the calculation of the composition is repeated with adjusted values of the estimated pressure, $p_c^{(n)}$, but the same temperature $T_c^{(1)}$. Since the effect of pressure on the formation enthalpy of the final gas mixture is usually not very large, the calculated pressure is, in most cases, fairly close to the correct pressure so that successive estimates may be obtained by the formula

$$p_{c,est}^{(n+1)} = p_{c,est}^{(n)} + X \cdot \left(p_{c,calc}^{(n)} - p_{c,est}^{(n)} \right),$$

WORKSHEET NO. 1

Procedure for Calculating the Mole Fractions, η_i, of a Combustion Gas in Equilibrium Containing the Species: H_2O, H_2, O_2, OH, O, and H

① $K^{(O)} = K_p^{(O)} \cdot P_c^{-1/2} = 0.145185$ $\quad T_c^{(1)} = 3000$ K $\quad T_m = 685.2$ K

② $K^{(H_2O)} = K_p^{(H_2O)} \cdot P_c^{1/2} = 17.063590$ $\quad P_c = 0.6$ atm $\quad P_m = 1.0042$ atm

③ $K^{(OH)} = 1.1967$ $\quad \frac{\nu_{O_2}^g}{\nu_{H_2}^g} = 0.5625$ $\quad m_m = 12.81024$ kg/kmol

④ $K^{(H)} = K_p^{(H)} \cdot P_c^{-1/2} = 0.203203$ $\quad M_m = 0.2298$ $\quad$ n = 1

Assume: $\sqrt{\eta_{O_2}^{(n)}} = 0.28$ → [1]

[1] · ② + 1 = [3]
[1] · ③ + 4 = [4]
$\left(\frac{[4]}{[3]}\right) \cdot 0.5 =$ [5]

$-\left[[2] + [1]^2\right] + 1 =$ [6]

$\left[\left\{\frac{[6]}{[3]} + [5]^2\right\}^{0.5} - [5]\right] =$ [7]

			m_i
[1] · [1]	$= \eta_{O_2}$ = 0.078400		32.000
[1] · ①	$= \eta_O$ = 0.040652 → [2]		16.000
[7] · [1] · ③	$= \eta_{OH}$ = 0.116158	[3]	17.008
[7] · ④	$= \eta_H$ = 0.070443	[4]	1.008
[7] · [7]	$= \eta_{H_2}$ = 0.120175	[5]	2.016
[5] · [1] · ②	$= \eta_{H_2O}$ = 0.574172	[6]	18.016
	$\sum \eta_i = 1.000000$		

$m_c = \sum \eta_i m_i = 15.792409$ kg/kmol

$$\Delta^{(n)} = \frac{\eta_{O_2}^g}{\eta_{H_2}^0} - \frac{\nu_{O_2}^g}{\nu_{H_2}^g} = \frac{\left([2] + [3] + [6]\right) \cdot 0.5 + [1]^2}{\left([3] + [4]\right) \cdot 0.5 + [5] + [6]} - \frac{\nu_{O_2}^g}{\nu_{H_2}^g} = 0.001066\ [7]$$

If [7] ≠ 0, Repeat Calculations with $\sqrt{\eta_{O_2}^{(2)}} = \sqrt{\eta_{O_2}^{(1)}}\left(1 - [7] \cdot 2\right) \rightarrow [1]$

If More Than Two Iterations are Required to Make $|[7]| < 0.001$, Use Linear Interpolation as Follows (For n ≥ 2):

$$\sqrt{\eta_{O_2}^{(n+1)}} = \sqrt{\eta_{O_2}^{(n)}} - \Delta^{(n)} \frac{\sqrt{\eta_{O_2}^{(n)}} - \sqrt{\eta_{O_2}^{(n-1)}}}{\Delta^{(n)} - \Delta^{(n-1)}} \rightarrow [1]$$

where $0.5 \leq X < 1$. The iterations are repeated until $\left| p_{c,calc}^{(n)} - p_{c,est}^{(n)} \right| < \epsilon$, where ϵ is again a small number which must be chosen properly. A rather accurate value of the pressure can be obtained by linear interpolation between two pressures for which the differences $p_{c,calc}^{(m)} - p_{c,est}^{(n)} \equiv \Delta^{(n)}$ and $p_{c,calc}^{(n-1)} - p_{c,est}^{(n-1)} \equiv \Delta^{(n-1)}$ are small. In this case we have

$$p_c = p_{c,est}^{(n-1)} - \Delta^{(n-1)} \cdot \frac{p_{c,est}^{(n)} - p_{c,est}^{(n-1)}}{\Delta^{(n)} - \Delta^{(n-1)}} .$$

To begin the calculations with temperature and pressure estimates which guarantee a rapid convergence to the correct values, we calculate first the adiabatic flame temperature (see Table 11) of the mixture (initial state m) at constant pressure when the flow is subsonic ($M_m < 1$) and at constant volume when the flow is supersonic ($M_m > 1$). For subsonic flow this temperature applies to the case that s.r. = 0 [see Eq. (65)] and for supersonic flow the constant volume $\left(\frac{v_c}{v_m} = 1\right)$ adiabatic flame temperature makes the speed ratio (s.r.) infinitely large. For subsonic flows the adiabatic flame temperature at constant pressure is only slightly larger than T_c, and p_c is only slightly less than p_m because heat addition to a subsonic flow has a mildly expansive effect, whereas for supersonic flows T_c is much higher than the adiabatic flame temperature at constant volume, and p_c is many times that of p_m because heat addition to a supersonic flow has a strongly compressive effect.

After a compatible pair of $\frac{T_c}{T_m}$ and $\frac{p_c}{p_m}$ values has been obtained from Eq. (69) by iteration, it is used to calculate the dimensionless speed of the initial gas, s.r., according to Eq. (65). If this calculated speed ratio (or its square) differs from the actual speed ratio of the initial gas, $\left(\frac{u_m^2}{R_m T_m}\right)$, all previous calculations must be repeated with an improved estimate, $T_c^{(n)}$, of the final temperature, together with a new value for p_c. For subsonic flows the speed ratio, s.r., is increased as $T_c^{(n)}$ is decreased and vice versa. Therefore, we have

$$T_{c,est}^{(n+1)} < T_{c,est}^{(n)} , \tag{71}$$

when

$$(s.r.)^2 < \frac{u_m^2}{R_m T_m} , \tag{72}$$

and vice versa. Since there are two solutions, it is necessary to calculate the Mach number, M_c, of the final flow to make sure that it is less than one. The solution with $M_c > 1$ has no physical significance because the transition from subsonic to supersonic flow by means of heat

Table 11. Calculation of adiabatic flame temperature

$\eta_{H_2} = 0.64$ $\eta_{O_2} = 0.36$ $p_m = 1.0042$ atm $T_m = 685.2$ K

$\mathcal{M}_m = 12.81024$ kg/kmol $\frac{h_f^{T_m}}{R_m T_m} = 8.063347$. For the case that $u_m = 0$ and $p_c = p_m$ we have $T_c = 3115.9$ K as shown by the table below:

	T (K)	$\frac{h_f^T}{R_m T_m}$	
	3100	6.43	
	3110	7.44	
$T_m = 3115.9 \rightarrow$			$\leftarrow \frac{h_f^{T_m}}{R_m T_m} = 8.063347$
	3120	8.47	
	3130	9.52	
	3140	10.58	

addition in a constant area duct, although mathematically possible, can occur only when an expansion shock wave is involved which entails, however, a spontaneous decrease in entropy.

For supersonic flows both solutions are physically possible. One solution represents supersonic flows ($M_c > 1$) for which the temperatures and pressures are only moderately higher than those of the adiabatic combustion at constant volume. For this solution the speed ratio is increased as $T_c^{(n)}$ is decreased, and vice versa, so that the relationships [Eq. (71) and (72)] apply here too. For the second solution leading to $M_c < 1$, because of a normal shock wave, the final temperature and pressure are much higher than those of the adiabatic flame temperature at constant volume. For this solution the speed ratio, s.r., is increased as the temperature, $T_c^{(n)}$, is increased, and vice versa. Therefore, iterations for this solution must be based on the conditions

$$T_{c,est}^{(n=1)} > T_{c,est}^{(n)} , \tag{73}$$

when

$$(s.r.)^2 < \frac{u_m^2}{R_m T_m} , \tag{74}$$

and vice versa. The iterations are continued until

$$\left|(s.r.)^2 - \frac{u_m^2}{R_m \cdot T_m}\right| < \epsilon \ ,$$

where again ϵ is a small number chosen in accordance with the accuracy desired and the limitations given by the thermodynamic data (formation enthalpies and equilibrium constants) used in the calculations. A rather accurate value of the final temperature can be obtained by linear interpolation between two temperatures for which the differences $(s.r.)^2 - \frac{u_m^2}{R_m T_m} \equiv \delta$ are small. In this case we can write

$$T_c = T_{c,est}^{(n-1)} - \delta^{(n-1)} \cdot \frac{T_{c,est}^{(n)} - T_{c,est}^{(n-1)}}{\delta^{(n)} - \delta^{(n-1)}} \ .$$

(2) In the second method, the details of which are given in Section 3, the calculation of the state of the unreacted mixture is bypassed. Therefore, it is more difficult to begin the calculations with a reasonable estimate of the final temperature and pressure. Consequently a larger number of calculations is required, as evidenced by the data shown in Fig. 14. The results of both techniques are tabulated in Table 12. An increase of the speed of the oxygen flow from 200 m/s to 222 m/s produces choking. The final conditions for u = 221 m/s are given in Table 13. The physically impossible solution involving the subsonic-supersonic transition is included to show how close this flow is to that at which the Mach number of the combustion gas is one ($M_c = 1$).

III. TRANSITION FROM DEFLAGRATION TO DETONATION

Most previous research[16-19] on three-dimensional detonation waves dealt with the decay of waves generated by ignitors having high power densities. Since these observations are not necessarily pertinent to the prediction of the transition from deflagration to detonation, experiments were carried out in the Aeronautical and Astronautical Research Laboratories of The Ohio State University to study the propagation of deflagrations in practically unconfined hydrogen-air mixtures. Hydrogen-air mixtures, contained between 0.004 inch polyethylene sheets draped over a metal frame, were ignited in the center by an electrically heated copper wire having a diameter of 0.003 inch. The energy transferred from this igniter to the combustible gas mixture was sufficiently low to allow the combustion process to start as a deflagration. Furthermore, no metal vapor or hot particles were propelled through the combustible gas mixtures, which in all experiments contained 29.5% hydrogen. The flames were photographed on Kodak 35mm Tri-X film by a FASTAX camera. According to Figs. 15 and 16 the flame speeds are given by the following

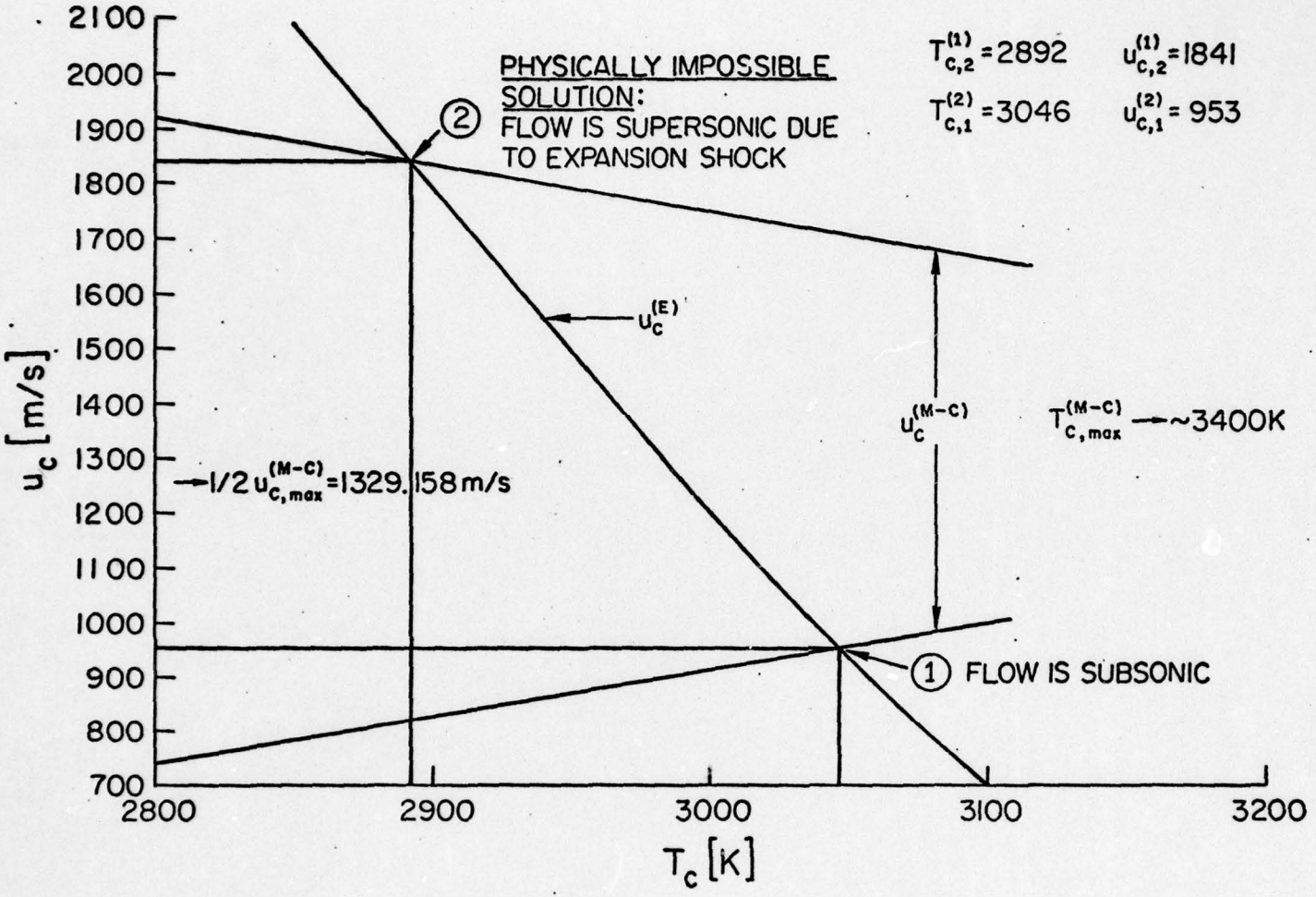

Fig. 14 - Relationships between final temperature, T_c, and gas speed, u_c, of burned gas in equilibrium; initial flow is subsonic (M_{H_2} = 0.0918, M_{O_2} = 0.2912)

Table 12. Mixing of a subsonic flow of oxygen with a subsonic flow of hydrogen followed by combustion

Initial State of Gases before Mixing	Mixing without Chemical Change	Combustion Gas in Complete Equilibrium
$u_{O_2} = 200$ m/s $u_{H_2} = 100$ m/s	$u_m = 179.56$ m/s	$u_c = 957.05$ m/s (953) [1]
$T_{O_2} = 1400$ K $T_{H_2} = 200$ K	$T_m = 685.2$ K	$T_c = 3044.5$ K (3046)
$p_{O_2} = 1$ atm $p_{H_2} = 1$ atm	$p_m = 1.0042$ atm	$p_c = 0.6881$ atm (0.690)
$M_{O_2} = 0.2912$ $M_{H_2} = 0.0918$	$M_m = 0.2298$	$M_c = 0.6801$
$\gamma_{H_2} = 1.4386$ $\gamma_{O_2} = 1.2972$	$\gamma_m = 1.3721$	$\gamma_c = 1.2182$
$\mathcal{M}_{O_2} = 32$ kg/kmol $\mathcal{M}_{H_2} = 2$ kg/kmol	$_m = 12.8$ kg/kmol	$c = 15.5718$ kg/kmol
$\eta_{H_2,1} = 0.64$	$\eta_{H_2,m} = 0.64$	$\eta_{H_2,c} = 0.1256$

(1) The values in parentheses were obtained by direct calculation (see Section 3).

Table 12. (continued)

Initial State of Gases before Mixing	Mixing without Chemical Change	Combustion Gas in Complete Equilibrium
$\eta_{O_2,1} = 0.36$	$\eta_{O_2,m} = 0.36$	$\eta_{O_2,c} = 0.0785$
		$\eta_{H_2O,c} = 0.5535$
		$\eta_{OH} = 0.1214$
		$\eta_{O} = 0.0441$
		$\eta_{H} = 0.0769$

Table 13. Mixing of subsonic flow of oxygen with a subsonic flow of hydrogen followed by combustion

Initial State of Gases before Mixing	Mixing without Chemical Change	Combustion Gas in Complete Chemical Equilibrium
$u_{O_2} = 221$ m/s $u_{H_2} = 100$ m/s	$u_m = 191.20$ m/s	$u_c = \begin{matrix}1282 \text{ m/s} \\ (1390)\end{matrix}$
$T_{O_2} = 1400$ K $T_{H_2} = 200$ K	$T_m = 686.0$ K	$T_c = \begin{matrix}2995 \text{ K} \\ (2976) \text{ K}\end{matrix}$
$P_{O_2} = 1$ atm $P_{H_2} = 1$ atm	$P_m = 1.0076$ atm	$P_c = \begin{matrix}0.535 \text{ atm} \\ (0.489) \text{ atm}\end{matrix}$
$M_{O_2} = 0.3217$ $M_{H_2} = 0.0918$	$M_m = 0.2445$	$M_c = \begin{matrix}0.9205 \\ (1.0028)\end{matrix}$

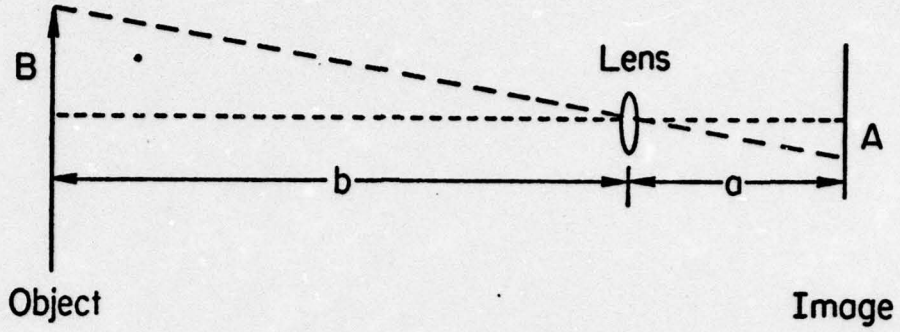

Fig. 15 - Geometrical representation of how an image is recorded on film

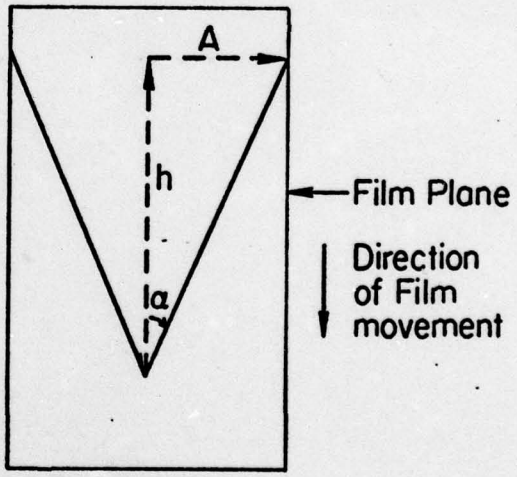

Fig. 16 - Trace of flame on rotating film strip

equation:

$$u_F = \left[\frac{b-F}{F}\right]\left[\frac{T_u}{T_b} \cdot \frac{\mathcal{M}_b}{\mathcal{M}_u}\right] \cdot \frac{dh}{dt} \cdot \tan\alpha \ ,$$

where b is the distance between the camera lens and the ignitor, F is the focal length of the lens, T_u the temperature of the unburned gas, T_b that of the burned gas, $\mathcal{M}_u$ and $\mathcal{M}_b$ the corresponding molecular masses, $\frac{dh}{dt}$ the film travel per unit time, and α the half-angle of the cone formed by the flame images on the film (see Fig. 17).

Measurements were made in bags containing 1, 2, and 4 m^3 of the hydrogen-air mixture; the results are shown in Fig. 18. Whereas the flame propagation rates in the 1 and 2 m^3 bags were quite reproducible, a fair amount of scatter prevailed in the 4 m^3 volume. The most significant observation, however, is the fact that there is a noticeable acceleration of the flame propagation (see also Fig. 17). This acceleration, although quite modest in the 1 m^3 bag, is large enough in the 4 m^3 bag that it may be assumed that a greater flame speed increase, possibly resulting in a detonation wave, would occur in much larger volumes of the combustible gas mixture. Unfortunately, experiments with larger bags cannot be carried out at this laboratory because of the strong compression waves which accompany these explosions and whose strengths increase rapidly with bag size.

Experiments to measure the pressure rise at various distances from the bags are in progress.

IV. QUENCHING OF DETONATION AND DEFLAGRATION WAVES

Because of the low gas speeds and small pressure changes produced by deflagration waves, the principal function of a flame arrestor consists of terminating the progress of the chemical reactions in the flame. On the other hand a detonation wave is followed by the high-speed flow of the hot combustion gas which is much more difficult to attenuate. Furthermore, this wave involves a large rise in pressure which must be dissipated by the arrestor in order to prevent ignition of the downstream gas by the shock compression. Therefore, arrestors designed to quench a detonation wave must not only stop the progress of the combustion process but they must also produce a drastic decay of the shock wave and prevent the hot gases, which traverse the arrestor, from igniting the downstream combustible gas mixture.

To study both effects independently, two different experimental investigations have been initiated. First a shock tube has been designed and constructed for measurements of the effectiveness of arrestors in bringing about a significant decay of the shock wave so that the wave

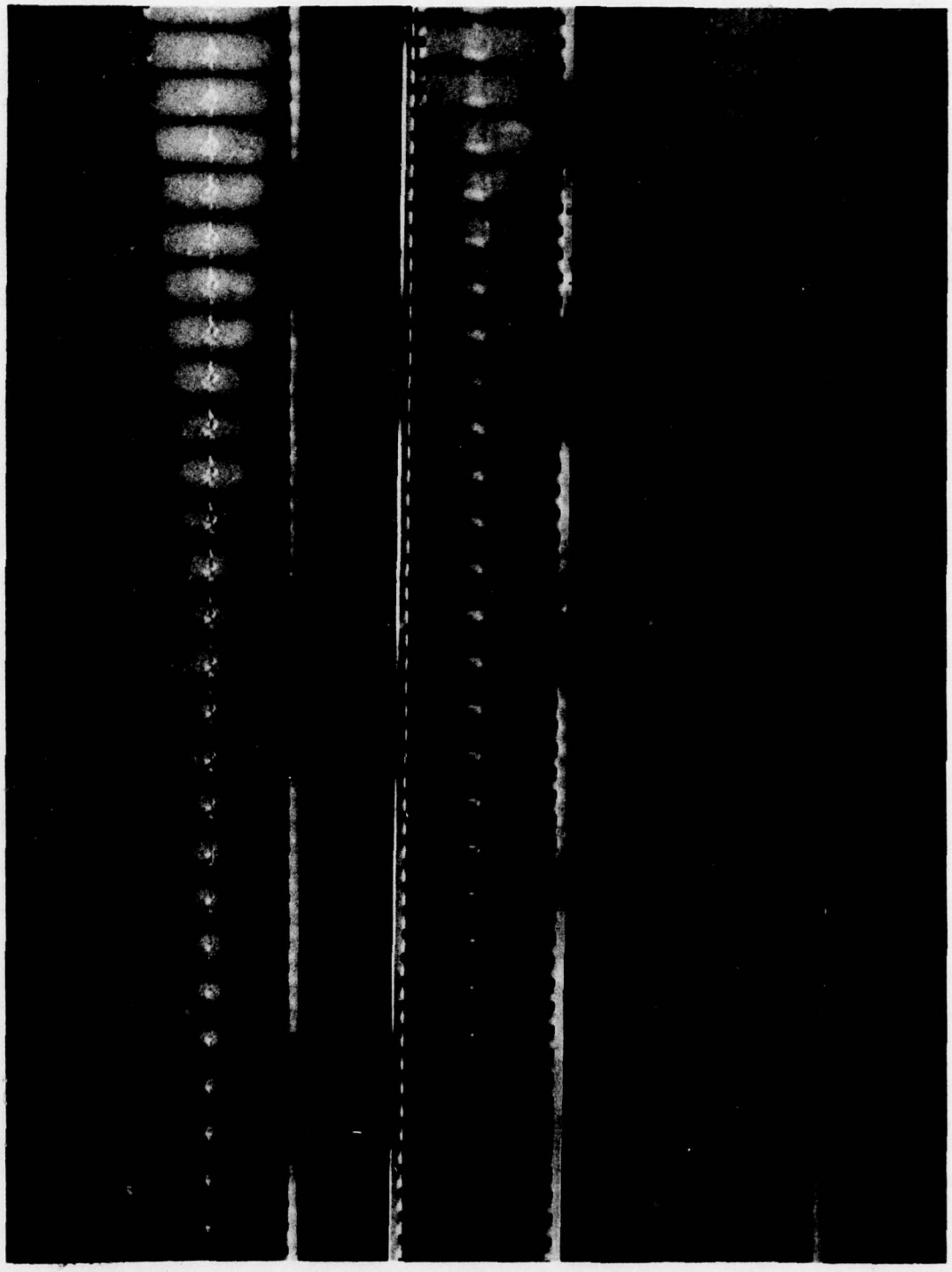

Fig. 17 - Sequence photographs (FASTAX) of flames in different size bags

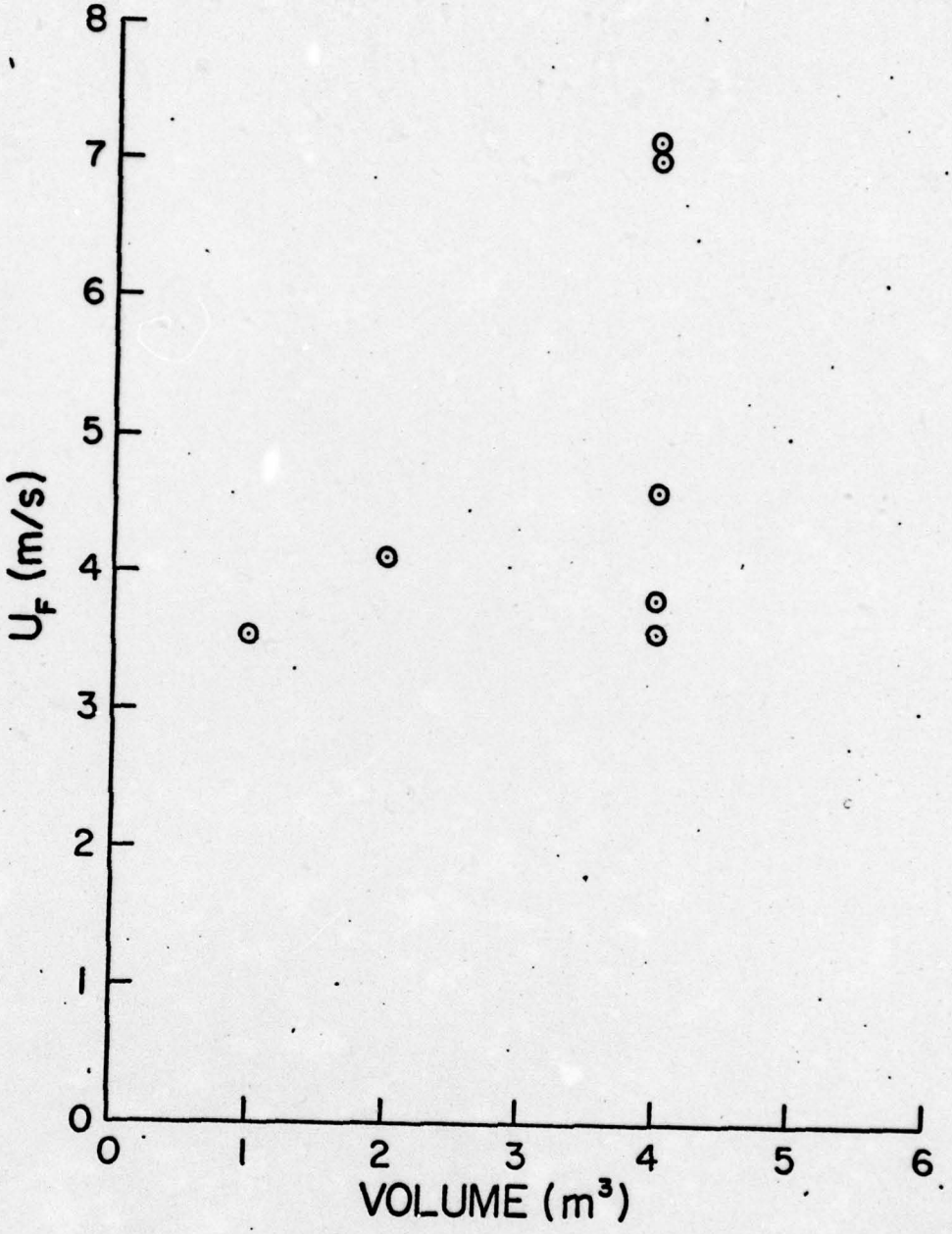

Fig. 18 - Flame speed as a function of bag size

emerging from the arrestor can no longer ignite the downstream gas. Progress on this investigation has been slow because several graduate students, after working on this problem, have decided to discontinue their studies toward an advanced degree.

Another apparatus (see schematic views shown in Figs. 19 and 20) has been designed and constructed for the study of flame quenching by arrestors made of different materials, having various porosities and configurations. The test section, as shown in Fig. 20, accommodates the arrestor and has a rectangular cross-section. It is equipped with large windows to photographically record the processes occurring at the ignitor surfaces. Eight photo transistors (Texas Instrument LS 400) will be used to determine the flame propagation rates. Several thermocouples will be placed in the upstream and downstream sections for temperature measurements. The pressures in both sections will be monitored by quartz crystal transducers. Photographic records will be obtained with a 35mm Fastax camera. The combustion will be initiated by two spark plugs fed by a 7.5 kV ignition transformer. It is planned to use hydrogen-air, methane-air, and propane-air mixtures for these experiments. Several arrestor materials have been given to us by the Air Force Aero Propulsion Laboratory. These samples include polyurethane foams of different pore sizes, and mesh and sponges made of aluminum and stainless steel.

In both types of experiments the initial gas mixtures are at rest. Future experiments are planned with flowing gas mixtures.

V. PERFORMANCE OF SUPERSONIC RAMJET

Previous calculations of the thrust specific fuel consumption of supersonic ramjets (see AFOSR-TR 76 0503) revealed that the best performance can be attained only with extremely high pressures in the combustion chamber unless operation at altitudes where $p_\infty < 10^{-4}$ atm is considered.

To investigate the effects of (1) less efficient diffusion processes, (2) the use of hydrocarbon fuel (propane) instead of hydrogen and (3) the mixing of fuel-air streams at different injection speeds and temperatures on the thrust specific fuel consumption of the engine additional calculations were made, the results of which are compiled in Table 14. According to these data highly efficient diffusers are not necessarily desirable when high flight speeds are considered because they lead to very high pressures in the combustion chamber. Although an inefficient diffusion process (e.g., a normal shock at the diffuser inlet) can be used to avoid the high static pressure in the combustion chamber, the losses caused by the rise in entropy of the air lead to very high values of the thrust specific fuel consumption. An additional increase in the thrust specific fuel consumption is produced when the temperature and the injection speed of the fuel differ greatly from the respective values of the air flow through the combustion chamber inlet.

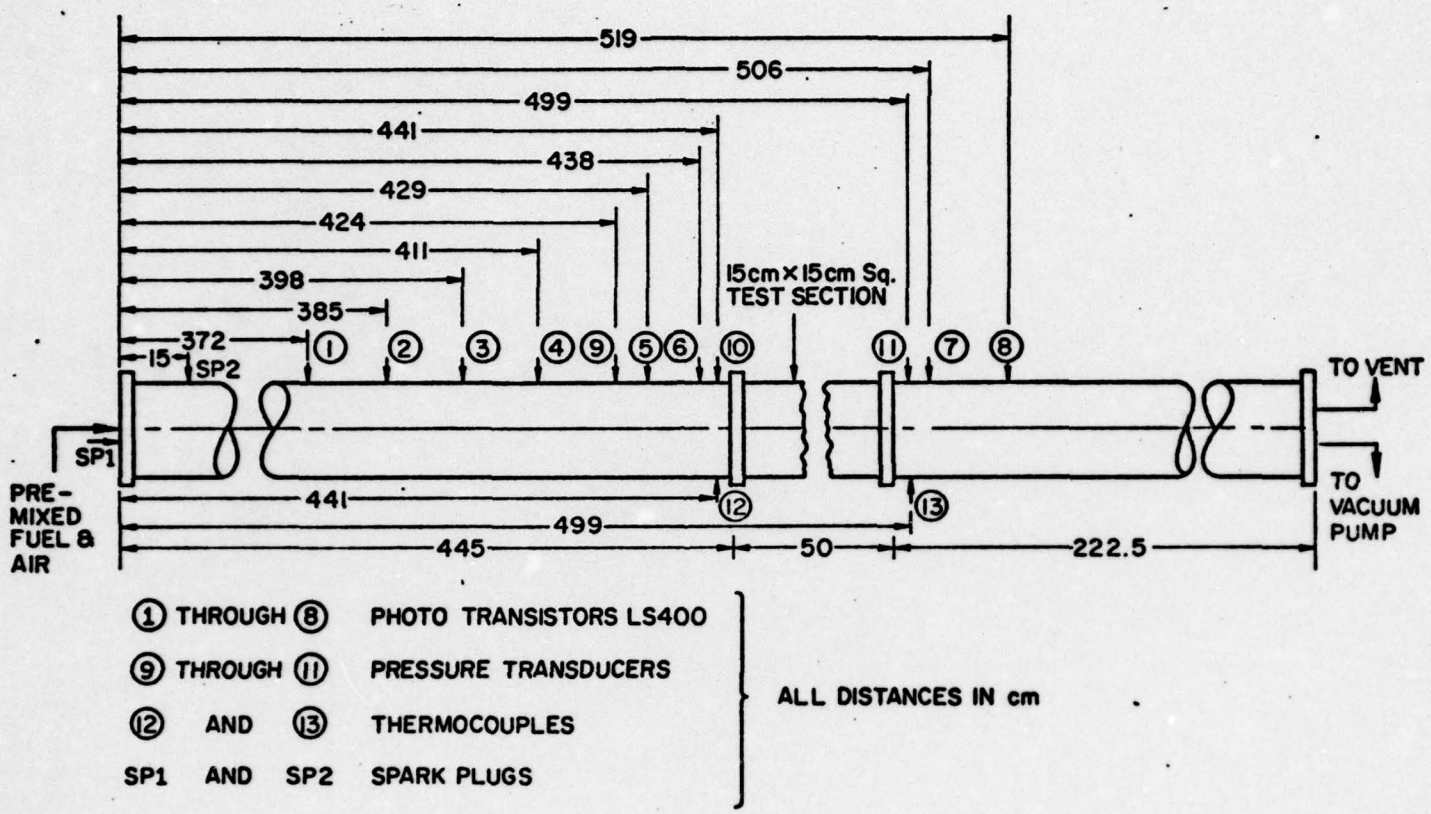

Fig. 19 - General arrangement of the 15 cm I.D. combustion tube to be used for flame quenching

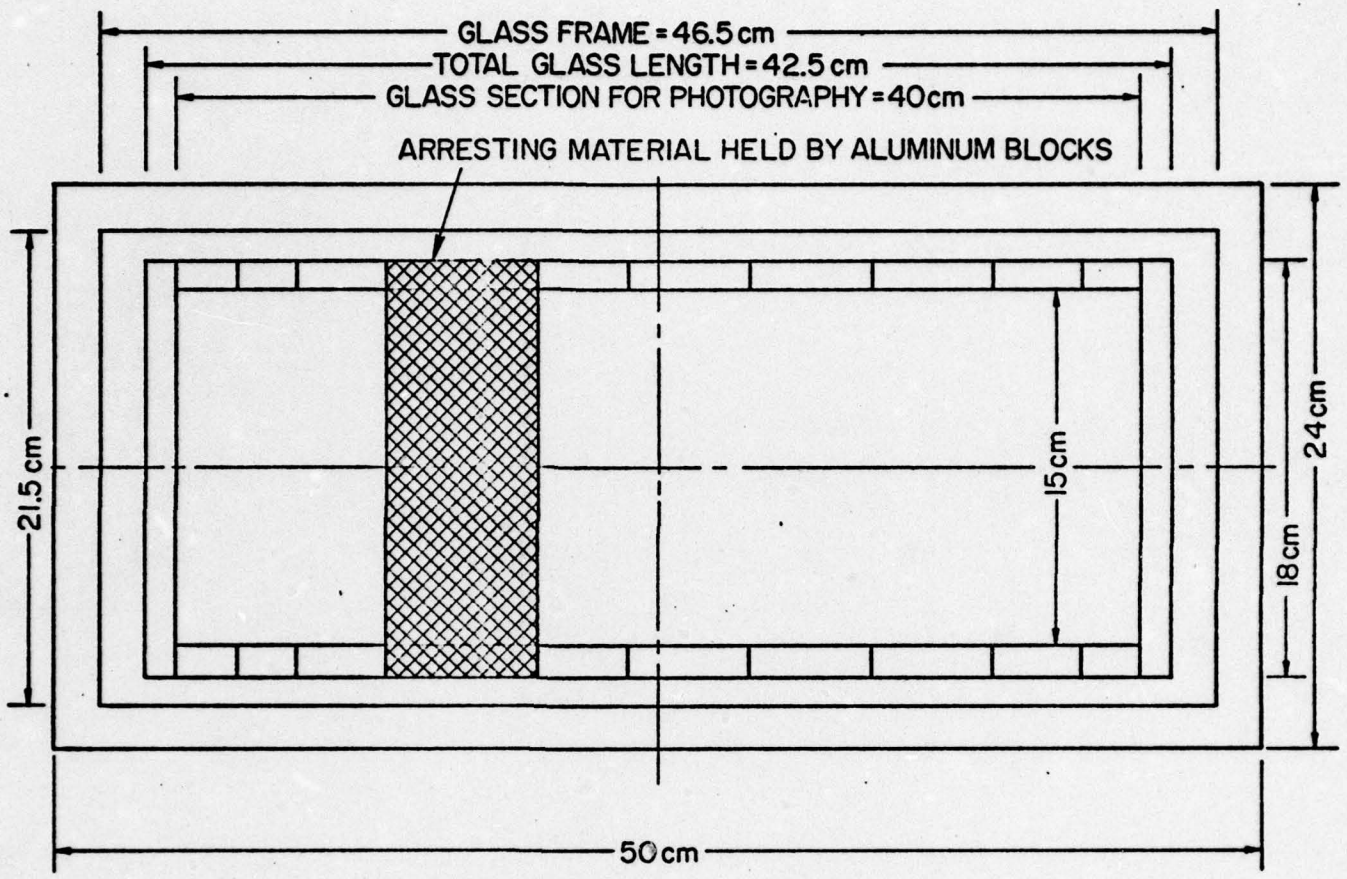

Fig. 20 - Test section detail (scale 1/2 full size)

Table 14. Thrust specific fuel consumption (F_{sfc}) of supersonic ramjets operated at various modes

Initial State of Atmospheric Air: T_∞ = 200 K and p_∞ = 0.01 atm

M_∞	Fuel-Air Mixture	Diffusion Process	Maximum Static Pressure in Engine (atm)	Mode of Mixing	F_{sfc} [(kg/h)/N]
10	$H_2 + \frac{1}{2}O_2 + 1.88N_2$	ds = 0 subsonic combustion	600 to 850	ideal: $T_{fuel} = T_{air}$, $Tu_{fuel} = u_{air}$	0.08
10	$H_2 + \frac{1}{2}O_2 + 1.88N_2$	ds = 0 supersonic combustion	weak detonation 61 atm / strong detonation 147 atm	ideal: $F_{fuel} = T_{air}$, $u_{fuel} = u_{air}$	0.10 / 0.10
10	$C_3H_8 + 5O_2 + 18.8N_2$	ds = 0	600 to 850	ideal: $F_{fuel} = T_{air}$, $u_{fuel} = u_{air}$	0.21
		N.S. at diffuser inlet	1.3		0.88
		N.S. at diffuser inlet	1.3	T_{fuel} = 300 K, u_{fuel} = 0	1.43
5	$H_2 + \frac{1}{2}O_2 + 1.88N_2$	ds = 0	5.5	ideal: $T_{fuel} = T_{air}$, $u_{fuel} = u_{air}$	0.07
5	$H_2 + \frac{1}{2}O_2 + 1.88N_2$	Normal shock at Diffuser inlet	0.3	ideal: $T_{fuel} = T_{air}$, $u_{fuel} = u_{air}$	0.12

REFERENCES

1. Edse, R., and Lawrence Jr., L. R., Combustion and Flame, 13, 5, 479 (1969).

2. Urtiew, P. A., and Oppenheim, A. K., Eleventh Symposium (International) on Combustion, p. 665. The Combustion Institute: Pittsburgh (1967).

3. Oppenheim, A. K., Manson, N., and Wagner, H. G. G., AIAA Journ. 1, 10, 2243 (1963).

4. Gaydon, A. G., and Wolfhard, H. G., Flames, p. 76, Chapman and Hall: London (1970).

5. Lewis, B., and von Elbe, G., Combustion Flames and Explosion of Gases, 2nd Ed. Academic Press: New York (1961).

6. Markstein, G. H., Sixth Symposium (International) on Combustion, p. 387. Reinhold: New York (1957).

7. Brinkley Jr., S. R., and Lewis, B., Seventh Symposium (International) on Combustion, p. 807. The Combustion Institute: Butterworths, London (1959).

8. Karlovitz, B., Selected Combustion Problems, p. 176. Butterworths: London (1954).

9. Zeldovitch, Y. B., J. Exp. Theoret. Phys. (U.S.S.R.), 10, 542 (1940). [Trans. in NACA Tech. Memo. 1261 (1950)]

10. von Neumann, J., "Theory of Detonation Waves," Office of Scientific Research and Development, Rep. 549 (1942).

11. Döring, W., Ann. Physik, 43, 421 (1943).

12. Fay, J. A., Eighth Symposium (International) on Combustion, p. 30. The Williams & Wilkins: Baltimore (1962).

13. Edwards, D. H., Twelfth Symposium (International) on Combustion, p. 819. The Combustion Institute: Pittsburgh (1969).

14. Martin, F. J., and White, D. R., Seventh Symposium (International) on Combustion, p. 856. The Combustion Institute: Butterworths, London (1959).

15. Sokolik, A. S., Self Ignition, Flame, and Detonation in Gases, p. 357. Izdatel'stvo Akedemi Nauk USSR, Moskva (1960). Translated from Russian by Israel Program for Scientific Translations, Jerusalem (1963).

16. Egerton, A. and Gates, S. F., "On Detonation of Gaseous Mixtures of Acetylene and of Pentane," Proc. Roy. Soc. Vol. 114 pp. 137-151 March 1927.

17. Egerton, A. and Gates, S. F., "On Detonation of Gaseous Mixtures at High Initial Pressures and Temperatures," Proc. Roy. Soc. Vol. 114 pp. 152-160 March 1927.

18. Sokolik, A. and Shtsholkin, K., "Detonation in Gaseous Mixtures," Acta Physicochim U.S.S.R., Vol. 7 pp. 581-596 1937.

19. Bollinger, L. E., Fong, M. C., and Edse, R., "Experimental Measurements and Theoretical Analysis of Detonation Induction Distances," ARS Journal, May 1961.


END
DATE
FILMED
3-77

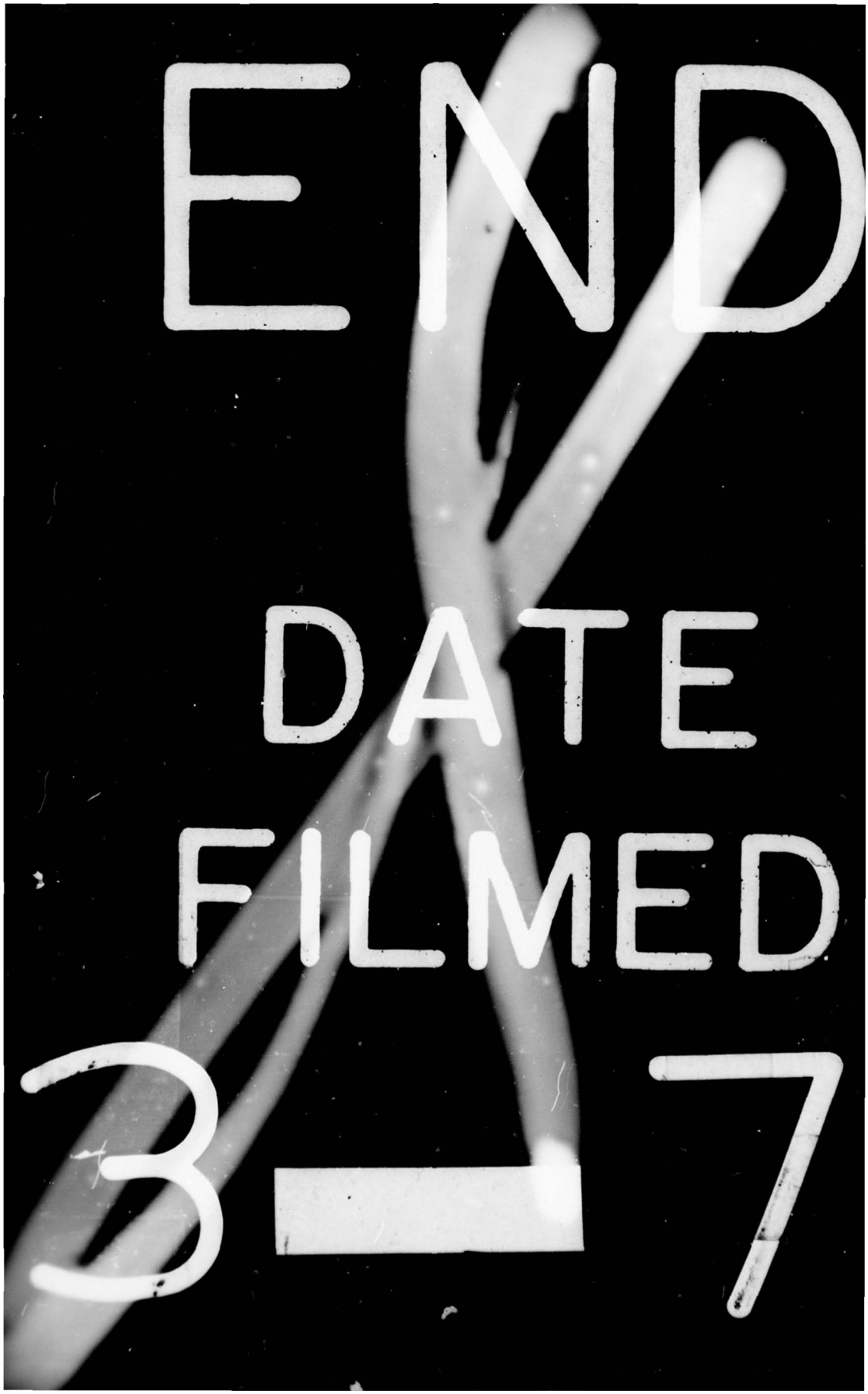
END
DATE
FILMED
3 7

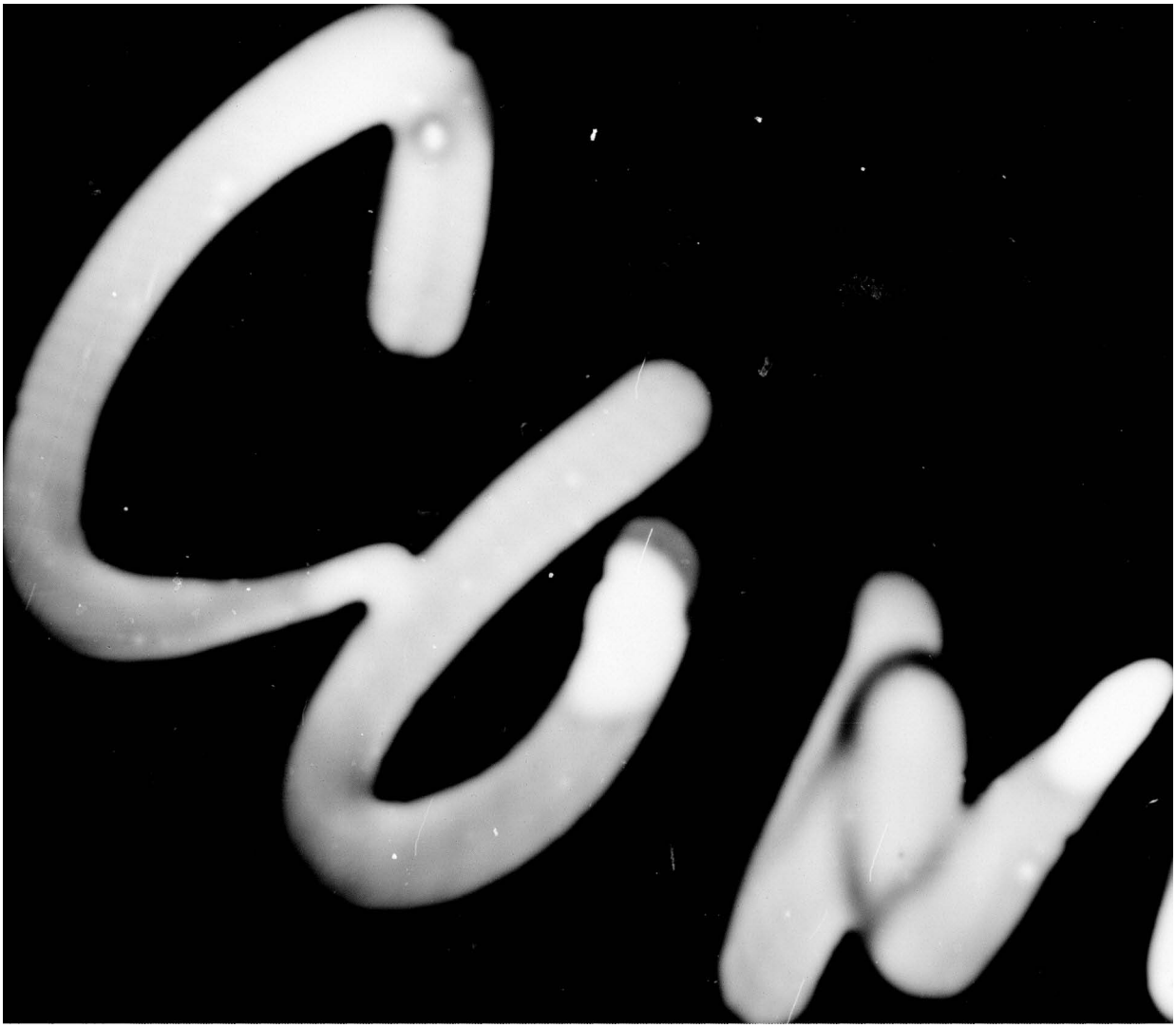

AD-A035 486 IGNITION COMBUSTION DETONATION AND QUENCHING OF REACTIVE MIXTURES(U) OHIO STATE UNIV RESEARCH FOUNDATION COLUMBUS R EDSE ET AL. SEP 76

UNCLASSIFIED AFOSR-TR-77-0059 AF-AFOSR-2511-73 F/G 21/2 NL

2/2

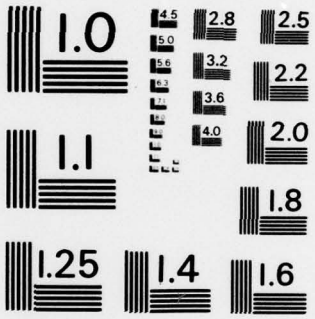

SUPPLEMENTARY

INFORMATION

Errata

AD-A035 486

Page 72 is blank.

DTIC-DDAC
30 Aug 84